Inorganic Chemistry

Article

pubs.acs.org/IC

Reversible Carbon–Carbon Bond Formation Induced by Oxidation and Reduction at a Redox-Active Cobalt Complex

Crisita Carmen Hojilla Atienza, Carsten Milsmann, Scott P. Semproni, Zoë R. Turner, and Paul J. Chirik*

Department of Chemistry, Princeton University, Princeton, New Jersey 08544, United States

Supporting Information

ABSTRACT: The electronic structure of the diamagnetic pyridine imine enamide cobalt dinitrogen complex, (^{iPr}PIEA)CoN_2 (^{iPr}PIEA = 2-(2,6-^{i}Pr$_2$–C_6H_3N═CMe)-6-(2,6-^{i}Pr$_2$–C_6H_3NC═CH_2)C_5H_3N), was determined and is best described as a low-spin cobalt(II) complex antiferromagnetically coupled to an imine radical anion. Addition of potential radical sources such as NO, PhSSPh, or Ph_3Cl resulted in C–C coupling at the enamide positions to form bimetallic cobalt compounds. Treatment with the smaller halocarbon, $PhCH_2Cl$, again induced C–C coupling to form a bimetallic bis(imino)pyridine cobalt chloride product but also yielded a monomeric cobalt chloride product where the benzyl group added to the enamide carbon. Similar cooperative metal–ligand addition was observed upon treatment of (^{iPr}PIEA)CoN_2 with CH_2═$CHCH_2Br$, which resulted in allylation of the enamide carbon. Reduction of Coupled-(^{iPr}PDI)CoCl (Coupled-(^{iPr}PDI)CoCl = [2-(2,6-^{i}Pr$_2$–C_6H_3N═CMe)-C_5H_3N-6-(2,6-^{i}Pr$_2$–C_6H_3N═CCH_2–)CoCl]$_2$) with $NaBEt_3H$ led to quantitative formation of (^{iPr}PIEA)CoN_2, demonstrating the reversibility of the C–C bond forming reactions. The electronic structures of each of the bimetallic cobalt products were also elucidated by a combination of experimental and computational methods.

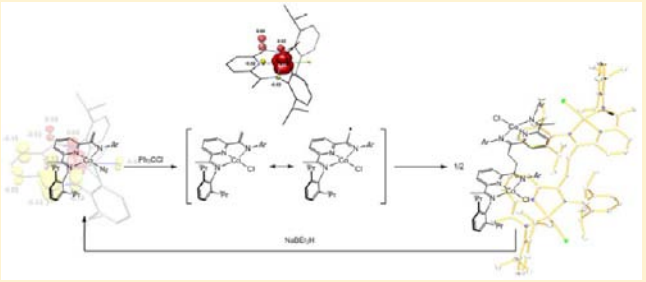

INTRODUCTION

The transition metal chemistry of so-called noninnocent and redox-active ligands continues to attract attention.[1,2] Ligand radical chemistry has now been identified in the function of certain metalloenzymes,[3−5] small molecule activation,[6] and group transfer reactions[7,8] as well as base metal catalysis.[9−11] The focus in most cases has been the *electronic* consequences of ligand-centered radicals on the overall function or reactivity of the metal complex.[12]

A more recent emphasis has been to exploit the redox activity to promote chemistry at the ligand.[13] Given the importance of carbon–carbon bond-forming reactions, it is not surprising that considerable emphasis has been placed on this specific bond construction.[14] Floriani and co-workers and more recently Nocera and co-workers have observed carbon–carbon bond cleavage resulting from ligand-centered redox changes in transition metal porphyrinogen complexes.[15,16] Wolczanski and co-workers have reported a rich C–C bond forming chemistry derived from first row transition metal complexes containing redox-active bis(2-pyridyl)azaallyl chelates.[17] The nonbonding orbitals of the azaallyl fragment are described as having equal ionic and covalent character that account for the dimerization of an iron amide compound[17] and bis(ligand) complexes of titanium.[18] This ligand-centered reactivity has been expanded to include bis(pyridine-imines) and has resulted in elegant examples of the simultaneous formation of three C–C bonds in complexes of nickel, cobalt, and chromium.[19]

Most recently, Holland and co-workers reported the reversible coupling of pyridine ligands in iron diketiminate complexes.[20] Spectroscopic and computational studies on the iron bis(pyridine) complexes established significant radical character on the basal pyridine ligand. Upon crystallization, a bimetallic iron complex was isolated resulting from C–C bond formation between two pyridine ligands. In solution, the monomeric variant was trapped with a triphenylmethyl radical and furnished a complex with a [Ph_3C] substituent in the 4-position of the reduced heterocycle. Irreversible C–C bond formation likely derived from ligand radical character has also been observed with pyridine and polypyridine ligands in reduced complexes of ruthenium,[21] tungsten,[22] yttrium,[23] and titanium.[24]

Bis(imino)pyridines are a well-established class of redox-active ligands.[25−28] Accordingly, Gambarotta and co-workers have demonstrated that the imine methyl groups of the aryl-substituted bis(imino)pyridine, ^{iPr}PDI (^{iPr}PDI = 2,6-(2,6-^{i}Pr$_2$–C_6H_3–N═CMe)$_2C_5H_3N$), undergo C–C bond formation by transfer hydrogenation in nickel complexes[29] or following deprotonation in manganese and iron compounds.[30,31] Carbon–carbon coupling of the pyridine ring has also been observed upon treatment of (^{iPr}PDI)$CrCl_3$ with $PhCH_2MgCl$.[30]

During the course of our investigations into the reduction chemistry of the bis(imino)pyridine cobalt chloride complex, (^{iPr}PDI)CoCl, our laboratory discovered that addition of NaO^{t}Bu resulted in formal deprotonation of one of the imine

Received: February 11, 2013
Published: April 18, 2013

   dx.doi.org/10.1021/ic400352r | *Inorg. Chem.* 2013, 52, 5403−5417

methyl groups to furnish (^{iPr}PIEA)CoN_2 (^{iPr}PIEA = 2-(2,6-$^{i}Pr_2$−C_6H_3N=CMe)-6-(2,6-$^{i}Pr_2$−C_6H_3NC=CH_2)-C_5H_3N; eq 1).[32] The latter will be depicted in its redox-innocent form in all equations until the data establishing its electronic structure have been presented. Formation of enamide ligands from deprotonation of bis(imino)pyridines is well-precedented among complexes of iron,[33] manganese,[30] chromium,[34] and the lanthanides.[35,36]

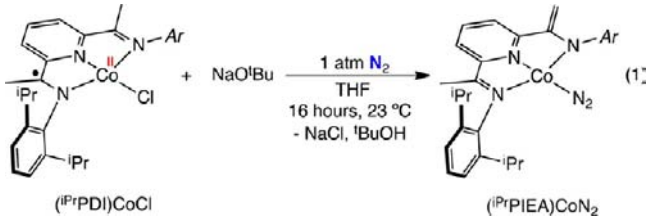

The isolation of (^{iPr}PIEA)CoN_2 prompted comparison to (^{iPr}PDI)CoN_2, a compound that is best described as a low-spin Co(I) complex with a bis(imino)pyridine-centered radical as the SOMO.[32] Related studies by Zhu and Budzelaar have examined the oxidative addition reactivity of (^{Ar}PDI)CoN_2 with various aryl halides and demonstrated the predominance of radical pathways, some of which result in chelate alkylation.[37−39] In the enamide variant, (^{iPr}PIEA)CoN_2, the remaining imino(pyridine) portion of the ligand preserves the possibility of redox activity[40,41] and therefore has prompted additional studies to elucidate the electronic structure of the compound along with exploration of its reactivity toward alkyl halides. Here, we describe these efforts and report a reversible C−C bond forming event that can be triggered by sequential one-electron oxidation and reduction.

RESULTS AND DISCUSSION

Molecular and Electronic Structure of (^{iPr}PIEA)CoN_2. Distortions to the bond distances of bis(imino)pyridines and related ligands are a useful diagnostic for evaluating redox activity.[27,42] Although (^{iPr}PIEA)CoN_2 was previously characterized by NMR and IR spectroscopies and combustion analysis, the solid state structure was not determined. The molecular structure of (^{iPr}PIEA)CoN_2 was determined by X-ray diffraction and is shown in Figure 1. Selected bond distances and angles are reported in Table 1. Also included in Table 1 are metrical parameters for (^{iPr}PIEA)Li(THF)[43] and (^{iPr}PIEA)Cr(THF)[35] for comparison.

As with the bis(imino)pyridine counterpart,[32] the geometry about the metal in (^{iPr}PIEA)CoN_2 is best described as planar. The imine methyl group can be distinguished from the methylene by both the C−C bond distances (imine methyl C(1)−C(2) = 1.475(3) Å and the enamide methylene (C(8)−C(9) = 1.400(3) Å) and the location of the hydrogen atoms. Bond contractions and elongations are often one of the most reliable indicators of redox activity.[5] The modification of the chelate renders comparison to bis(imino)pyridines unreliable; rather, parameters for related α-iminopyridines are more appropriate.[40,41] The C_{imine}−N_{imine} bond distance of 1.364(2) Å is elongated from the neutral ligand value of 1.28 Å established by Wieghardt and co-workers but is shorter than the value of 1.46 Å defined for an imino(pyridine) dianion. The data are most consistent with one-electron reduction (1.34 Å). Likewise, the C_{imine}−C_{ipso} distance of 1.429(3) Å is contracted compared to the value of 1.47 Å for the neutral form of the ligand and longer than the value of 1.35 Å accepted for the dianion. It is most comparable to the value of 1.41 Å accepted for the monoreduced ligand. The bond distortions of the chelate in the cobalt compound are also comparable to the values observed in a related chromium complex where the ligand is monoreduced.[34] Thus, the crystallographic data are most consistent with a cobalt(II) center antiferromagnetically coupled to an imino(pyridine) radical anion.

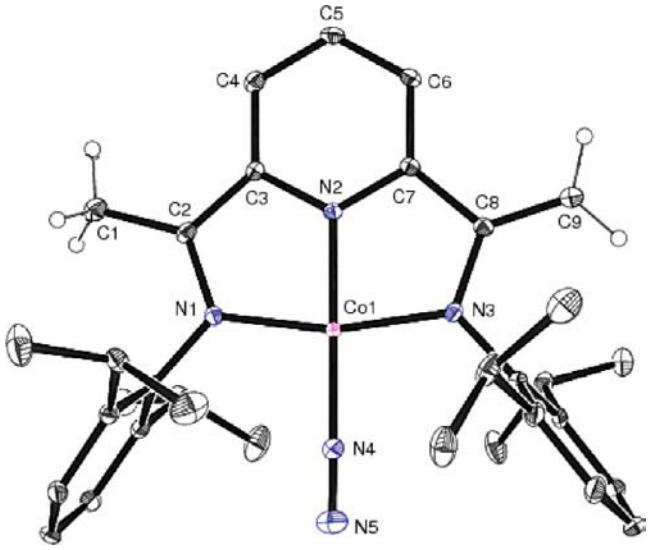

Figure 1. Solid state structure of (^{iPr}PIEA)CoN_2 at 30% probability ellipsoids. Hydrogen atoms, except for those on C(1) and C(9), are omitted for clarity.

Table 1. Experimental and Calculated Bond Distances (Å) and Angles (deg) for (^{iPr}PIEA)CoN_2[a]

	experimental	calculated	(^{iPr}PIEA)Li(THF)	(^{iPr}PIEA)Cr(THF)
M(1)−N(1)	1.8679(17)	1.911	2.364(4)	2.020(3)
M(1)−N(2)	1.8216(16)	1.850	2.033(4)	1.946(3)
M(1)−N(3)	1.8586(17)	1.878	2.013(5)	2.020(3)
M(1)−N(4)	1.8176(19)	1.848		
N(1)−C(2)	1.364(2)	1.354	1.290(3)	1.382(4)
N(2)−C(3)	1.372(2)	1.368	1.347(3)	1.382(4)
N(2)−C(7)	1.364(3)	1.343	1.337(3)	1.361(4)
N(3)−C(8)	1.373(3)	1.393	1.355(3)	1.375(4)
C(1)−C(2)	1.475(3)	1.501	1.500(3)	1.447(5)
C(2)−C(3)	1.429(3)	1.430	1.491(3)	1.424(5)
C(7)−C(8)	1.468(2)	1.484	1.496(3)	1.440(5)
C(8)−C(9)	1.400(3)	1.359	1.369(3)	1.421(5)
N(4)−N(5)	1.110(3)	1.100		
N(1)−M(1)−N(2)	82.27(7)	82.11	72.54(14)	78.90(11)
N(1)−M(1)−N(3)	165.08(7)	165.49	151.9(2)	157.86(11)
N(1)−M(1)−N(4)	97.48(8)	97.24		
N(2)−M(1)−N(3)	82.83(7)	83.38	79.32(15)	79.0(11)
N(2)−M(1)−N(4)	179.34(8)	179.35		
N(3)−M(1)−N(4)	97.40(8)	97.27		
M(1)−N(4)−N(5)	179.2(2)	179.87		

[a]Metrical parameters for (^{iPr}PIEA)Li(THF)[43] and (^{iPr}PIEA)Cr(THF)[34] are included for comparison.

The electronic structure of (^{iPr}PIEA)CoN_2 was also studied computationally with full molecule calculations at the B3LYP level of DFT.[44] A broken symmetry (BS) (1,1) solution[45] was found to be lowest in energy and successfully reproduced the experimentally determined metrical parameters (Table 1).

dx.doi.org/10.1021/ic400352r | Inorg. Chem. 2013, 52, 5403−5417

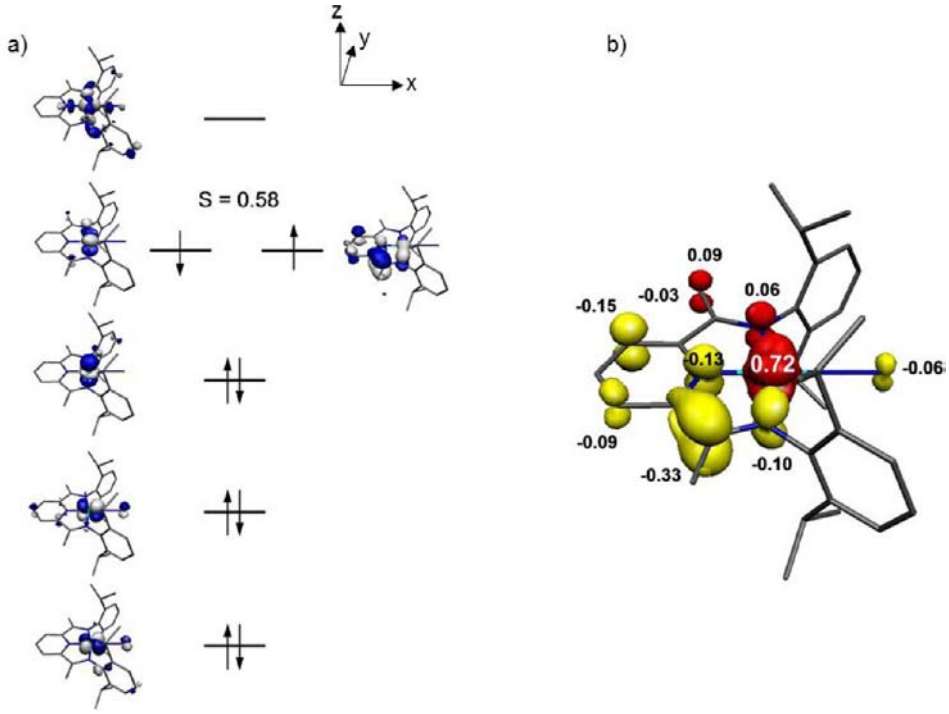

Figure 2. (a) Qualitative molecular orbital diagram for (^{iPr}PIEA)CoN_2 from a geometry-optimized B3LYP DFT calculation. (b) Spin density plot obtained from Mulliken population analysis (red, positive spin density; yellow, negative spin density).

Scheme 1

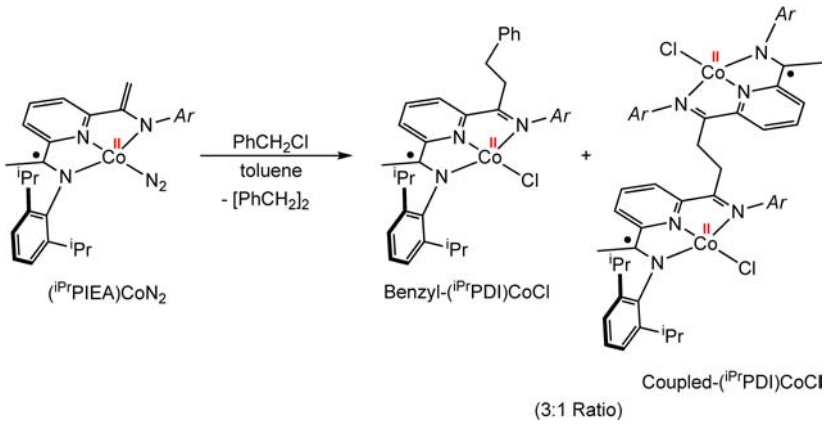

As illustrated in Figure 2, this solution produces a frontier molecular orbital diagram expected for a four-coordinate, planar transition metal complex. The essentially d_{yz} cobalt orbital is engaged in the antiferromagnetic coupling interaction (S = 0.58, S = spatial overlap of the magnetic orbitals) with an a'' orbital of the imino(pyridine) portion of the chelate. Notably, the spin on the α-imino(pyridine) is opposite the cobalt-based spin and the radical character on the enamide carbon.

Reactivity of (^{iPr}PIEA)CoN_2 with Organic Halides. The reactivity of (^{iPr}PIEA)CoN_2 with alkyl halides was examined to explore the role of the redox active imino(pyridine) and the unsaturation of the enamide portion of the ligand in oxidative processes. Recently our laboratory reported C−C oxidative addition of biphenylene to the bis(imino)pyridine iron dinitrogen compound, (^{iPr}PDI^{2-})Fe^{II}(N_2), and established the overall two-electron process occurred with concomitant one-electron loss at both the iron center and the bis(imino)-pyridine chelate.[46] In bis(imino)pyridine cobalt chemistry, Zhu and Budzelaar demonstrated that oxidative addition of alkyl halides to (^{Ar}PDI^{-})Co^{I}(N_2) resulted in two separate cobalt-based one-electron oxidations to form mixtures of (^{Ar}PDI^{-})-Co^{II}X and (^{Ar}PDI^{-})Co^{II}R.[37,38] Similar reactivity has been observed by our group upon the addition of alkyl halides and certain C−O bonds to (^{iPr}PDI)FeN_2.[47,48]

Addition of one equivalent of benzyl chloride to an approximately 36 mM benzene-d_6 solution of (^{iPr}PIEA)CoN_2 in benzene-d_6 produced a 3:1 mixture of two cobalt compounds (Scheme 1). We note that, because of the mixture of products, the equations presented in Schemes 1 and 2 are not balanced. The major product was identified as the modified bis(imino)-pyridine cobalt chloride complex, Benzyl-(^{iPr}PDI)CoCl (Benzyl-(^{iPr}PDI) = 2-(2,6-^{i}Pr$_2$−C_6H_3N═CMe)-6-(2,6-^{i}Pr$_2$−C_6H_3N═C-(CH$_2$)$_2$Ph)C_5H_3N), where the benzyl group had added across the enamide to reconstitute the imine. The minor product was identified based on comparison to independent synthesis (*vide infra*) as a bimetallic cobalt compound, Coupled-(^{iPr}PDI)CoCl

dx.doi.org/10.1021/ic400352r | *Inorg. Chem.* 2013, 52, 5403−5417

(Coupled-(^{iPr}PDI)CoCl = [2-(2,6-^{i}Pr$_2$−C$_6$H$_3$N═CMe)-C$_5$H$_3$N-6-(2,6-^{i}Pr$_2$−C$_6$H$_3$N═CCH$_2$−)CoCl]$_2$), arising formed from C−C bond formation at the enamide positions. Attempts to perturb the product ratio by changing the ratio of the reactants, slow addition of reagents, use of different solvents, or varying the temperature had little effect.

Because Coupled-(^{iPr}PDI)CoCl was the minor product from benzyl chloride addition to (^{iPr}PIEA)CoN$_2$, an independent synthesis was sought to isolate the compound and facilitate full characterization. A more hindered alkyl chloride was selected to inhibit C−C bond formation with the alkyl radical at the enamide position of the chelate. Addition of one equivalent of Ph$_3$CCl to a toluene solution of (^{iPr}PIEA)CoN$_2$ resulted in clean and quantitative formation of Coupled-(^{iPr}PDI)CoCl along with a stoichiometric quantity of the Gomberg dimer, Ph$_3$CCH(CHCH)$_2$CCPh$_2$ (eq 2).

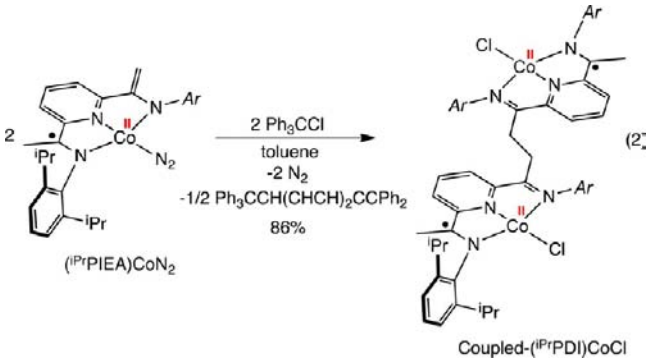

The benzene-d_6 ^{1}H and ^{13}C NMR spectra of Coupled-(^{iPr}PDI)CoCl exhibit the number of resonances consistent with C_s symmetry and two equivalent cobalt subunits. The *p*-pyridine and imine methyl resonances were located at 9.67 ppm and 0.34 ppm, respectively, slightly shifted from the 9.54 ppm and 0.05 ppm values for (^{iPr}PDI)CoCl.[49] The methylene bridge appears as a singlet at 2.58 ppm, which is shifted by +0.30 ppm from the imine methyl resonance of free ^{iPr}PDI.[50] The ^{1}H NMR resonances of Coupled-(^{iPr}PDI)CoCl are consistent with other (^{Ar}PDI)CoX (X = halide, alkyl, hydride) compounds where the *p*-pyridine and imine methyl protons are significantly shifted compared with the free chelate. A similar trend has been observed with (^{iPr}PDI)Fe(N$_2$), where the protons on the chelate plane exhibit unusual ^{1}H NMR resonances.[26,51]

The solid-state structure of Coupled-(^{iPr}PDI)CoCl was determined by X-ray diffraction, and a representation of the molecule is shown in Figure 3. Selected metrical parameters are reported in Table 2. Two half molecules were present in the asymmetric unit, and half of the dimer was generated by symmetry. One of the two THF molecules in the asymmetric unit was modeled as a cyclopentane because definitive assignment of the oxygen atom was not possible due to disorder. The geometry about each cobalt center is best described as idealized planar with the sum of the bond angles totaling to 359.98(48)° and 360.05(44)°, respectively. The metrical parameters of the bis(imino)pyridine ligand are consistent with one-electron reduction (see Table 2) and comparable to those found in (^{iPr}PDI)CoCl (C_{imine}−C_{ipso} = 1.444(5) and 1.435(5) and N_{imine}−C_{imine} = 1.322(5) and 1.317(5)).[49,52]

The electronic structure of Coupled-(^{iPr}PDI)CoCl was also examined by DFT calculations. A single point calculation at the B3LYP level was performed on the truncated Coupled-(^{iPr}PDI)CoCl, where the diisopropylphenyl substituents on the imine nitrogen were replaced with methyl groups. The single point calculation and the truncations were made to minimize computational expense. The calculation converged to a BS(2,2) solution with opposite spins on the chelate and the metal center in each monomeric unit (Figure 4). Thus, both the

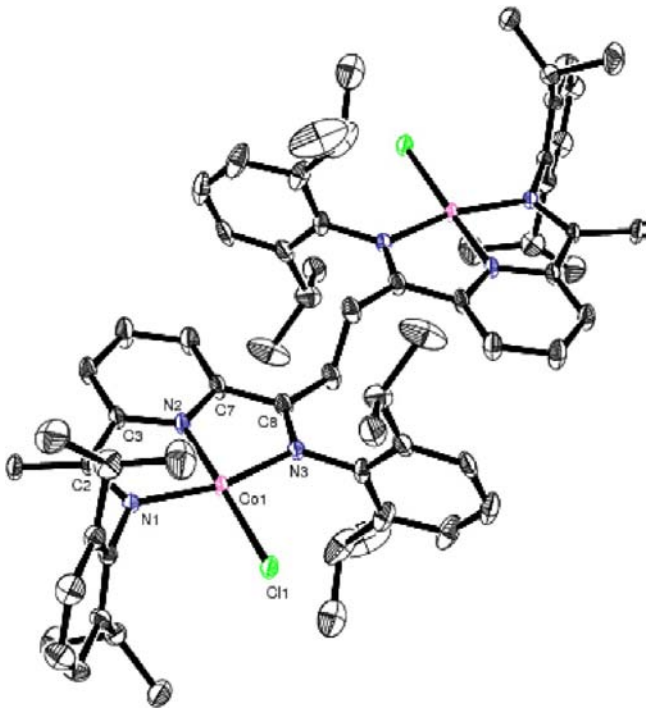

Figure 3. Solid state structure of Coupled-(^{iPr}PDI)CoCl at 30% probability ellipsoids. Only one of the two half molecules in the asymmetric unit is shown. One half of the molecule was generated by symmetry. THF molecules and hydrogen atoms were omitted for clarity.

Table 2. Selected Bond Distances (Å) and Angles (deg) for Coupled-(^{iPr}PDI)CoCl,[a] Coupled-(^{iPr}PDI)CoBr,[b] Coupled-(^{iPr}PDI)CoSPh, and Coupled-(^{iPr}PDI)CoNO

	Coupled-(^{iPr}PDI)CoCl	Coupled-(^{iPr}PDI)CoBr	Coupled-(^{iPr}PDI)CoSPh	Coupled-(^{iPr}PDI)CoNO
Co(1)−N(1)	1.934(3)	1.920(2)	1.927(2)	1.9646(16)
Co(1)−N(2)	1.793(3)	1.803(2)	1.816(2)	1.8877(18)
Co(1)−N(3)	1.918(3)	1.909(2)	1.935(2)	1.9550(16)
Co(2)−N(4)	1.927(3)	1.932(2)		
Co(2)−N(5)	1.798(3)	1.799(2)		
Co(2)−N(6)	1.916(3)	1.928(2)		
N(1)−C(2)	1.307(5)	1.316(4)	1.325(3)	1.316(3)
N(3)−C(8)	1.320(5)	1.322(3)	1.324(3)	1.339(3)
N(4)−C(35)	1.313(5)	1.316(4)		
N(6)−C(41)	1.325(4)	1.322(3)		
C(2)−C(3)	1.442(5)	1.443(4)	1.430(4)	1.448(3)
C(7)−C(8)	1.438(5)	1.439(4)	1.428(4)	1.425(3)
C(35)−C(36)	1.454(5)	1.441(4)		
C(40)−C(41)	1.432(5)	1.437(4)		
N(1)−Co(1)−N(2)	81.20(13)	81.30(10)	81.00(9)	78.99(7)
N(2)−Co(1)−N(3)	81.88(13)	81.70(10)	80.65(9)	79.46(7)
N(4)−Co(2)−N(5)	81.67(12)	81.06(10)		
N(5)−Co(2)−N(6)	81.53(12)	81.93(10)		

[a]The values listed are for the two half molecules in the asymmetric unit. [b]The two cobalt subunits in the dimer are crystallographically inequivalent.

dx.doi.org/10.1021/ic400352r | Inorg. Chem. 2013, 52, 5403−5417

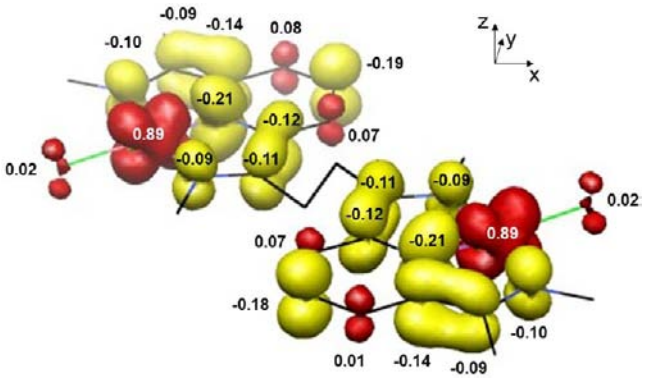

Figure 4. Spin density plot obtained from Mulliken population analysis of a truncated Coupled-(^{iPr}PDI)CoCl (red, positive spin density; yellow, negative spin density).

metrical parameters and the computational studies support low spin cobalt(II) complexes with antiferromagnetic coupling to a bis(imino)pyridine radical anion similar to monomeric (^{Ar}PDI)CoX (X = halide, alkyl) previously reported in the literature.[53]

The scope of the dimerization was further explored with other chlorine sources. Addition of Me_3SiCl, $PbCl_2$, 4-chlorotoluene, or $PhICl_2$ to a benzene-d_6 solution of (^{iPr}PIEA)CoN_2 all yielded Coupled-(^{iPr}PDI)CoCl. In the case of Me_3SiCl, a slow reaction was observed and only 60% conversion after 16 h at ambient temperature. Partial conversion was also observed under similar conditions with $PbCl_2$; $PhICl_2$ proved more reactive as complete consumption of (^{iPr}PIEA)CoN_2 occurred after 1 h at ambient temperature. Although Coupled-(^{iPr}PDI)CoCl was observed as the major product, unidentified side products were also formed. For 4-chlorotoluene, no conversion was observed at ambient temperature, and partial formation of Coupled-(^{iPr}PDI)CoCl along with multiple side products was observed upon heating to 80 °C for several hours. Thus, Ph_3CCl is the preferred reagent for synthesis of Coupled-(^{iPr}PDI)CoCl.

The oxidative addition of allylic halides was also explored. The relative stability of the allyl radical was attractive in an attempt to favor formation of monomeric, C_s-symmetric bis(imino)pyridine cobalt complexes from cooperative metal–ligand addition. Addition of one equivalent of CH_2=$CHCH_2Br$ to an approximately 36 mM solution of (^{iPr}PIEA)CoN_2 in benzene-d_6 in a J. Young tube furnished a mixture of two cobalt products in a 3:1 ratio (Scheme 2). Analysis of the volatile products of the reaction by ^{1}H NMR spectroscopy revealed formation of 1,5-hexadiene, presumably resulting from coupling of allyl radicals. The major cobalt product was identified as Allyl-(^{iPr}PDI)CoBr (Allyl-(^{iPr}PDI) = 2-(2,6-^{i}Pr$_2$–C_6H_3N=CMe)-6-(2,6-^{i}Pr$_2$–C_6H_3N=C(CH_2)$_2$CH=CH_2)-C_5H_3N) arising from cooperative metal–ligand addition. Diagnostic ^{1}H NMR resonances observed in benzene-d_6 are consistent with a diamagnetic, C_s symmetric bis(imino)pyridine cobalt bromide. The free allylated bis(imino)pyridine ligand has been previously synthesized and offered a useful reference for NMR shifts.[54] The minor product was identified as the bimetallic bis(imino)cobalt bromide complex, Coupled-(^{iPr}PDI)CoBr.

The ratio of cobalt products from allyl bromide addition could be perturbed by dilution. Performing the reaction with an approximately 5.6 mM solution of (^{iPr}PIEA)CoN_2 in toluene resulted in exclusive formation of Coupled-(^{iPr}PDI)CoBr (Scheme 2). Crystals suitable for X-ray diffraction were isolated from a concentrated benzene solution. The ^{1}H and ^{13}C NMR spectroscopic properties of Coupled-(^{iPr}PDI)CoBr are similar to Coupled-(^{iPr}PDI)CoCl, the details of which can be found in the Experimental Section.

The solid state structure of Coupled-(^{iPr}PDI)CoBr is presented in Figure 5, and selected metrical parameters are presented in Table 2. The geometry about each cobalt center is idealized planar with the sum of the bond angles around the metal centers totaling to 360.10(34)° and 360.32(34)°, respectively. The metrical parameters of the bis(imino)pyridine ligand are consistent with one electron chelate reduction,[26,27] suggesting two Co(II) centers (Table 2).

Attempts were made to extend cooperative metal–ligand additions to alkyl halides. Treatment of a benzene-d_6 solution of (^{iPr}PIEA)CoN_2 with bromoethane resulted in partial (approximately 70%) conversion to Coupled-(^{iPr}PDI)CoBr with concomitant formation of butane. Decreasing the ratio of CH_3CH_2Br to (^{iPr}PIEA)CoN_2 to 0.5:1 reduced the conversion to Coupled-(^{iPr}PDI)CoBr. No cobalt ethyl or hydride complexes were detected by ^{1}H NMR spectroscopy. Thus, the stability of the hydrocarbyl radical plays a role in the addition to the enamide carbon where more stable radicals favor C–C formation with the chelate.

Carbon–Carbon Bond Formation Promoted by Addition of Ph_2S_2 and NO. The generality of the C–C coupling process to form bimetallic cobalt complexes upon addition of reagents poised to promote one-electron chemistry with (^{iPr}PIEA)CoN_2

Scheme 2

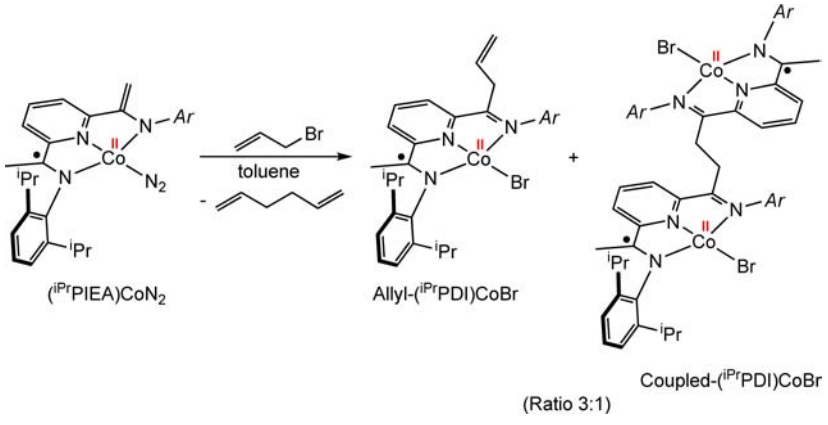

dx.doi.org/10.1021/ic400352r | Inorg. Chem. 2013, 52, 5403–5417

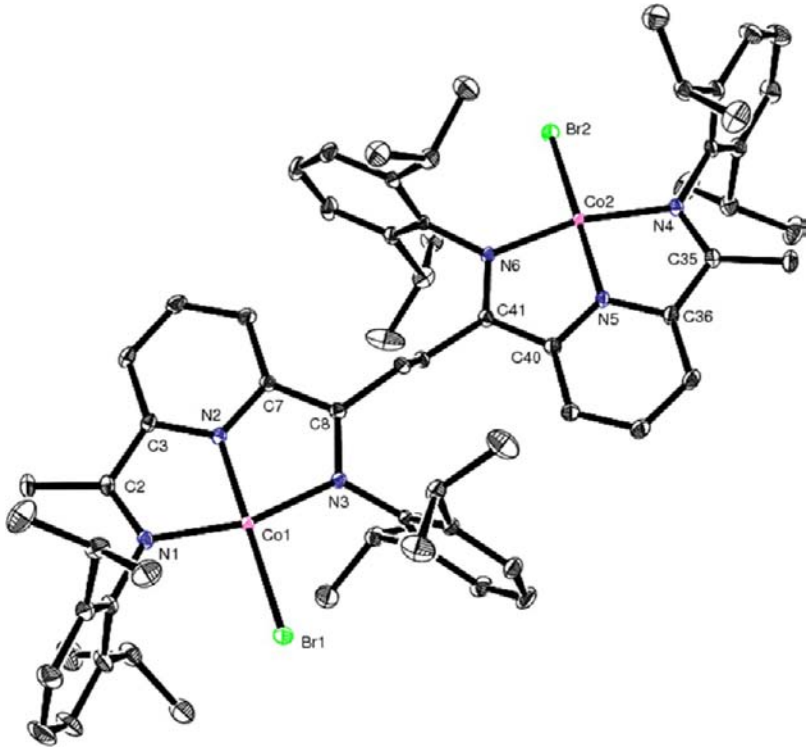

Figure 5. Molecular structure of Coupled-(^{iPr}PDI)CoBr at 30% probability ellipsoids. Benzene molecules and hydrogen atoms were omitted for clarity.

were explored. Addition of 0.5 equiv of Ph_2S_2 to a toluene solution of (^{iPr}PIEA)CoN_2 resulted in isolation of a dark pink, crystalline solid identified as Coupled-(^{iPr}PDI)CoSPh based on NMR spectroscopy, X-ray diffraction, and combustion analysis (eq 3).

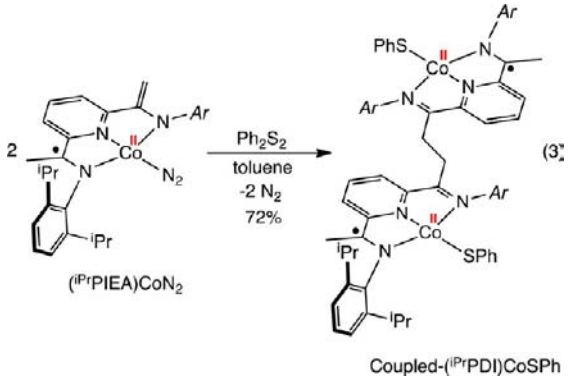

As with the corresponding chloride and bromide complexes, the two monomeric units of Coupled-(^{iPr}PDI)CoSPh are equivalent by ^{1}H and ^{13}C NMR spectroscopy, and the spectra exhibited the number of peaks consistent with a C_s-symmetric molecule. The *p*-pyridine resonance appears as a pseudo triplet at 9.28 ppm and the N_{imine}-CCH_3 and N_{imine}-CCH_2 protons are observed as singlets at 0.36 ppm and 2.62 ppm, respectively.

The solid-state structure of Coupled-(^{iPr}PDI)CoSPh was determined by X-ray diffraction, and a representation of the molecule is shown in Figure 6. Selected bond distances and bond angles are reported in Table 2. The phenyl sulfide ligand is slightly lifted from the idealized metal-chelate plane by 12.46(7)°. The metrical parameters of the bis(imino)pyridine ligand are consistent with one-electron reduction (Table 2),

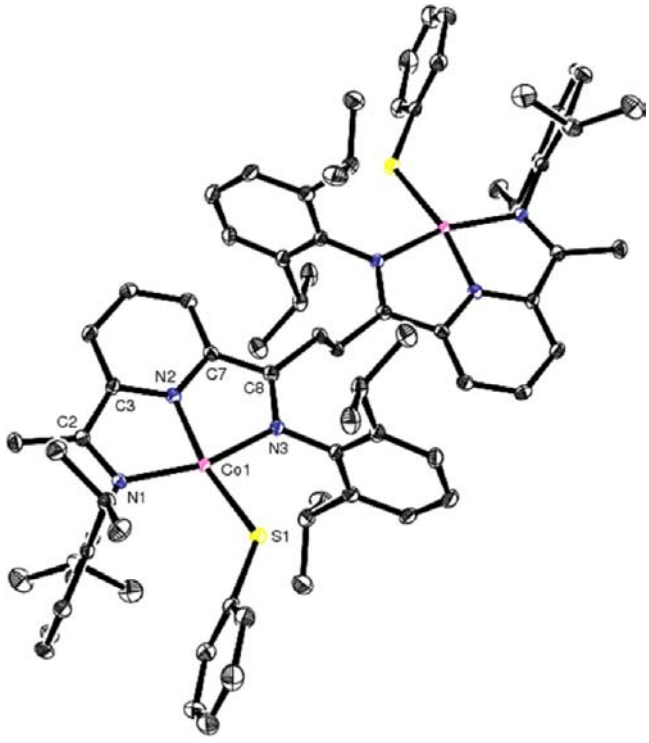

Figure 6. Molecular structure of Coupled-(^{iPr}PDI)CoSPh at 30% probability ellipsoids. One half of the molecule was generated by symmetry. Benzene molecules and hydrogen atoms were omitted for clarity.

and the electronic structure of Coupled-(^{iPr}PDI)CoSPh is best described as low-spin Co(II) antiferromagnetically coupled to a monoreduced chelate.

dx.doi.org/10.1021/ic400352r | *Inorg. Chem.* 2013, 52, 5403−5417

Similar C−C coupling and formation of a bimetallic bis(imino)pyridine cobalt complex were observed upon addition of one equivalent of nitric oxide to (^{iPr}PIEA)CoN$_2$ (eq 4). A dark pink crystalline solid was isolated in 96% yield that exhibited a diagnostic NO stretch centered at 1712 cm^{-1} in the benzene-d_6 solution IR spectrum. This value is comparable to the NO stretching frequencies observed with linear cobalt nitrosyl complexes in a tetrahedral ligand field (ν_{NO} = 1620−1710 cm^{-1})[55−57] and with the related planar bis(imino)-pyridine iridium nitrosyl complex, (^{iPr}PDI)IrNO (ν_{NO}, KBr = 1759 cm^{-1}).[58]

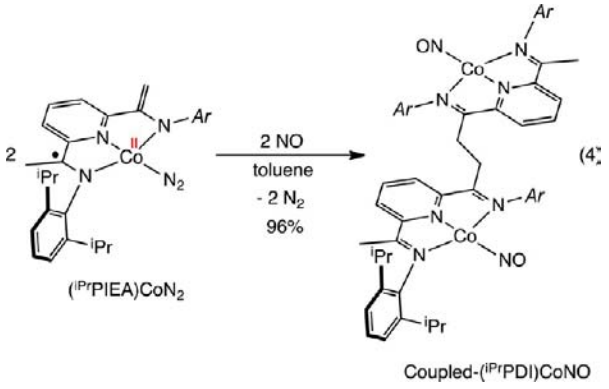

The benzene-d_6 solution ^{1}H and ^{13}C NMR spectra of Coupled-(^{iPr}PDI)CoNO exhibit the number of resonances for two equivalent C_s-symmetric bis(imino)pyridine cobalt sub-units. The ^{1}H resonances more closely resemble the chemical shifts of the free bis(imino)pyridine ligand[50] than reported (^{Ar}PDI)CoX (X = halide, alkyl) complexes,[53] suggesting a different electronic structure. For example, the *p*-pyridine is observed as a pseudo triplet at 7.21 ppm and the two doublets for the *m*-pyridine hydrogens were located at 6.97 and 7.46 ppm. The terminal NCCH_3 and bridging NCCH_2 appear as singlets at 2.06 and 3.56 ppm, respectively.

The solid-state structure of Coupled-(^{iPr}PDI)CoNO was determined by X-ray diffraction, and a representation of the molecule is shown in Figure 7. Selected bond distances and bond angles are reported in Table 2. Unlike the other bimetallic bis(imino)pyridine cobalt complexes reported in this work, the metal center is slightly lifted from the idealized chelate plane (Figure 8). The nitrosyl ligand is nearly linear with a Co−N−O angle of 167.96(18)°. The Co−N and N−O bond distances are 1.6376(19) Å and 1.189(2) Å, respectively, and are well within the range of other structurally characterized linear cobalt nitrosyl complexes.[53−55]

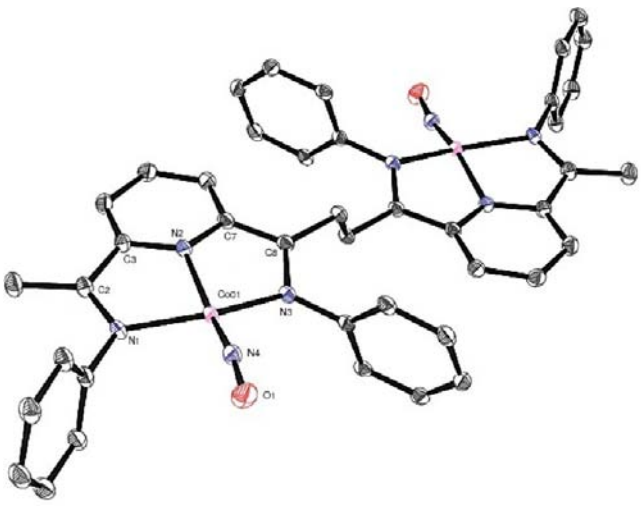

Figure 7. Molecular structure of Coupled-(^{iPr}PDI)CoNO at 30% probability ellipsoids. One half of the molecule was generated by symmetry. Isopropyl groups, toluene molecules, and hydrogen atoms omitted for clarity.

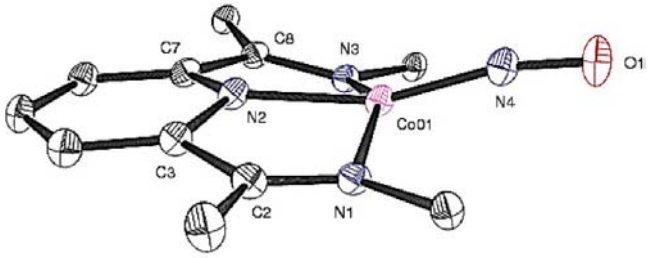

Figure 8. Truncated view of Coupled-(^{iPr}PDI)CoNO highlighting the distortion of the nitrosyl ligand from the metal chelate plane. Aryl groups, toluene molecules, and hydrogen atoms omitted for clarity.

The metrical parameters of the bis(imino)pyridine ligand are consistent with redox-activity and participation in the overall electronic structure of the compound. The C_{imine}−C_{ipso} distance in the terminal imine group is contracted to 1.448(3) Å, while the N_{imine}−CCH_3 bond length is elongated to 1.316(3) Å. These values are most consistent with a bis(imino)pyridine radical anion. The C_{imine}−C_{ipso} and N_{imine}−C_{imine} bond distances of the bridging imine groups are 1.425(3) Å and 1.339(3) Å, respectively. These values closely match the bond lengths observed with (^{iPr}PDI)CoN$_2$ (1.341(2) and 1.429(2) Å, respectively),[32] which has been described as having a monoreduced, radical anion chelate. The presence of a redox-active bis(imino)pyridine and nitrosyl ligand makes oxidation state assignment of the metal challenging. Historically, a linear nitrosyl has been assigned as a +1 ligand,[55,59] although in many instances such a description is either incomplete or inappropriate.[60] For this reason, the Enemark−Feltham notation has been developed, whereby a metal-nitrosyl is classified as {M-NO}^{n} where n is the sum of metal d electrons and the nitrosyl π^* electrons.[61] In this notation, Coupled-(^{iPr}PDI)-CoNO would be denoted as {Co-NO}^{9}.

To gain additional insight into the electronic structure of Coupled-(^{iPr}PDI)CoNO, the monomeric variant, (^{iPr}PDI)-CoNO, was synthesized by addition of one equivalent of NO gas to (^{iPr}PDI)CoN$_2$.[62] Recrystallization from a 3:1 pentane/toluene mixture furnished dark pink crystals identified as (^{iPr}PDI)CoNO in 86% yield (eq 5).

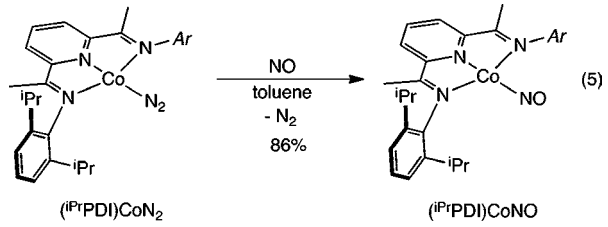

Diamagnetic (^{iPr}PDI)CoNO exhibited a strong NO band centered at 1712 cm^{-1} in the benzene-d_6 solution IR spectrum, consistent with a linear nitrosyl ligand. The benzene-d_6

dx.doi.org/10.1021/ic400352r | Inorg. Chem. 2013, 52, 5403−5417

^{1}H NMR spectrum of the compound exhibits the number of peaks consistent with a C_{2v}-symmetric molecule. The *p*-pyridine is observed as a triplet at 6.98 ppm and the *m*-pyridine as a doublet at 7.45 ppm. The imine methyl appears as a singlet at 2.05 ppm. These values are similar to those observed with Coupled-(^{iPr}PDI)CoNO, suggesting identical electronic structures.

The solid-state structure of (^{iPr}PDI)CoNO was determined by X-ray diffraction, and a representation of the molecule is presented in Figure 9. Selected bond distances and bond angles are reported in Table 3. The nitrosyl ligand is disordered over two positions giving distinct Co−N distances of 1.737(6) and 1.643(14) Å and N−O bond lengths of 1.101(7) and 1.167(16) Å. The Co−N−O angles are 166.4(5) and 169.1(10)°. The C_{imine}−C_{ipso} distances are contracted to 1.433(3) and 1.428(4) Å, and the N_{imine}−C_{imine} bonds are elongated to 1.322(3) and 1.324(3) Å, which indicate chelate reduction.

The electronic structure of (^{iPr}PDI)CoNO was studied by broken symmetry DFT calculations using the B3LYP functional. Because of the disorder in the solid-state structure of (^{iPr}PDI)CoNO, quantitative comparison between the observed and calculated Co−N−O bond lengths and angles is problematic. However, the DFT optimized structure for the compound is still in reasonable agreement with the crystallographic data for the portion of the molecule where disorder is absent and the experimental bond lengths are reliable (Table 3).[63] A qualitative molecular orbital diagram and spin-density plot derived from the calculations are presented in Figure 10. The BS(1,1) solution establishes a monoreduced bis(imino)pyridine chelate which is antiferromagnetically coupled to {Co(NO)}^{9}. As typically observed in metal-nitrosyl complexes, the Co−NO bond is highly covalent, which makes oxidation state assignments difficult.[60] The Co and NO contributions to the molecular orbitals are listed in Figure 10. Because the contribution to the Co−NO magnetic orbital is largely from the nitrosyl π^* orbital, the electronic structure of (^{iPr}PDI)CoNO can be best described as (PDI$^-$)Co^I(NO$^\bullet$) where the cobalt adopts a low-spin d^8 electronic configuration as expected for a planar Co(I) ion. This description is further corroborated by the spin density plots obtained from Mulliken population analysis (Figure 10).

Table 3. Selected Experimental and Computational Metrical Parameters for (^{iPr}PDI)CoNO

	exptl.	calcd.
Co(1)−N(1)	1.902(2)	1.979
Co(1)−N(2)	1.839(2)	1.875
Co(1)−N(3)	1.905(2)	1.977
Co(1)−N(4A)	1.737(6)	1.681
Co(1)−N(4B)	1.643(14)	
N(1)−C(2)	1.322(3)	1.324
N(2)−C(3)	1.369(3)	1.370
N(2)−C(7)	1.378(3)	1.371
N(3)−C(8)	1.324(3)	1.327
C(2)−C(3)	1.433(3)	1.446
C(7)−C(8)	1.428(4)	1.444
N(4A)−O(1A)	1.101(7)	1.173
N(4B)−O(1B)	1.167(16)	
N(1)−Co(1)−N(2)	80.09(10)	80.10
N(1)−Co(1)−N(3)	159.02(9)	158.10
N(1)−Co(1)−N(4A)	99.9(2)	100.30
N(1)−Co(1)−N(4B)	99.2(4)	
N(2)−Co(1)−N(3)	80.01(10)	80.10
N(2)−Co(1)−N(4A)	168.8(3)	174.00
N(2)−Co(1)−N(4B)	169.8(5)	
N(3)−Co(1)−N(4A)	100.9(2)	100.30
N(3)−Co(1)−N(4B)	99.2(4)	
Co(1)−N(4A)−O(1A)	166.4(5)	156.2
Co(1)−N(4A)−O(1A)	169.1(10)	

Burger and co-workers have previously reported the synthesis and crystallographic characterization of the bis(imino)pyridine iridium nitrosyl congener, (^{iPr}PDI)IrNO.[58] The NO stretching frequency of 1759 cm^{-1} is similar to the cobalt complex reported here. The N_{imine}−C_{imine} bond distances of 1.336(6) and 1.328(6) Å are consistent with one-electron reduction and suggest a similar electronic structure to (^{iPr}PDI)CoNO. However, the C_{imine}−C_{ipso} distances are

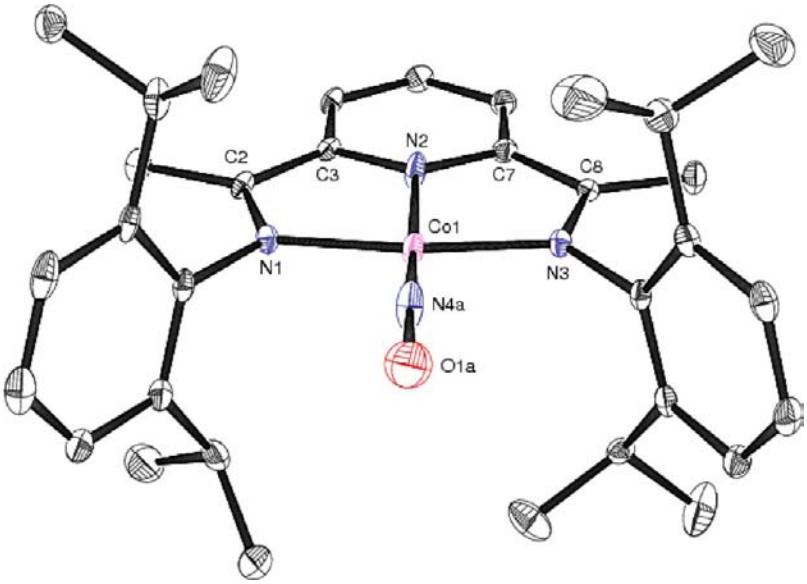

Figure 9. Molecular structure of (^{iPr}PDI)CoNO at 30% probability ellipsoids. Hydrogen atoms and one orientation of the disordered NO were omitted for clarity.

dx.doi.org/10.1021/ic400352r | Inorg. Chem. 2013, 52, 5403−5417

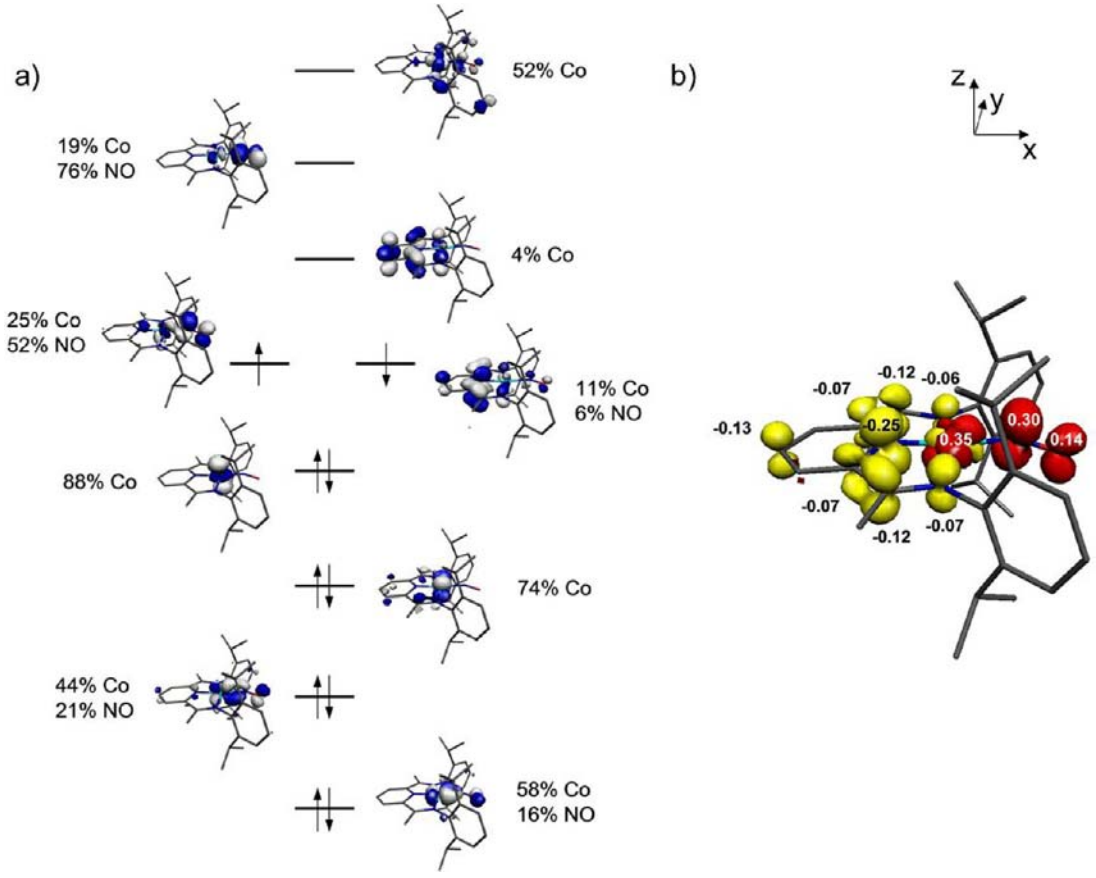

Figure 10. (a) Qualitative molecular orbital diagram for (^{iPr}PDI)CoNO from a geometry-optimized B3LYP DFT calculation. (b) Spin density plot obtained from Mulliken population analysis (red, positive spin density; yellow, negative spin density).

significantly contracted (1.387(7) and 1.395(7) Å) and are well within the accepted range for closed-shell two-electron reduction of the bis(imino)pyridine,[27,64] suggesting a more complicated electronic structure than the {Ir-NO}^{9} formalism would indicate.

Based on experimental and computational data, Burger and co-workers concluded that the iridium complex is best described as (PDI^{2-})Ir^{I}(NO^{+}).[65] Thus, while both the first and third row metal complexes are best described as being in the M(I), d^8 configuration, the redox state of the bis(imino)-pyridine and hence the nitrosyl ligand are different. In both cases, the preservation of the d^8 arrangement in the planar ligand field is a likely important determinant in the overall electron structure. For the iridium congener, a closed shell [PDI]$^{2-}$ is favored which renders the nitrosyl ligand in a formal [NO]$^{+}$ oxidation state. This is likely a consequence of the heavier transition metal preferring closed-shell electronic configurations with the pyridine diimine acting like a more classical π-acceptor (redox noninnocent).[1,66] By contrast, the first row congener (^{iPr}PDI)CoNO prefers a redox-active configuration arising from one electron reduction of the bis(imino)pyridine.

The difference in these two electronic structures is likely a result of the relative diffusivity and associated reduction potentials (i.e., ionization energies)[67] of the metal d orbitals. Redox noninnocence, when the bis(imino)pyridine acts as a π-acceptor, arises from the bonding situation where there is strong overlap between metal and ligand orbitals resulting in an energetically separated M−L bonding and antibonding pair. In the case of a redox-active, singlet biradical solution, as is observed with (^{iPr}PDI)CoNO, overlap between metal 3d orbitals and the bis(imino)pyridine π^* orbtials is diminished, resulting in a more accessible triplet state, which is in part a consequence of poor energetic separation of metal−ligand bonding and antibonding orbitals. Considering the relative diffusivity of iridium 5d and cobalt 3d orbitals, it is therefore unsurprising that a classical π-acid description is observed with the third row metal and that a single biradical state is observed with the light congener.[68] It is important to note that even when the overall electronic structures of two complexes appear similar, in this case two diamagnetic M(I) compounds, the redox states of the component redox-active ligands can be different.

On the basis of the observations that halides and pseudohalides such as PhS induce dimerization to bimetallic bis(imino)pyridine cobalt complexes upon addition to (^{iPr}PIEA)CoN$_2$, a tentative mechanism is proposed in Scheme 3. Unfortunately, the rapid rate of these reactions coupled with the lack of observables prevents much in the way of experimental support for the proposed pathway. The most plausible first step of the sequence involves formation of the cobalt−halogen/pseudohalogen bond. The introduction of an X-type ligand into coordination sphere of the metal likely alters the electronic structure of the complex and generates significant radical character on the enamide methylene position. In these instances where a long-lived hydrocarbon radical is present as in the case of benzyl or allyl, C−C bond formation results and yields a monomeric, C_s symmetric bis(imino)pyridine cobalt alkyl complex. In the absence of a suitable radical, dimerization occurs and yields the observed bimetallic cobalt compounds.

dx.doi.org/10.1021/ic400352r | Inorg. Chem. 2013, 52, 5403−5417

Scheme 3

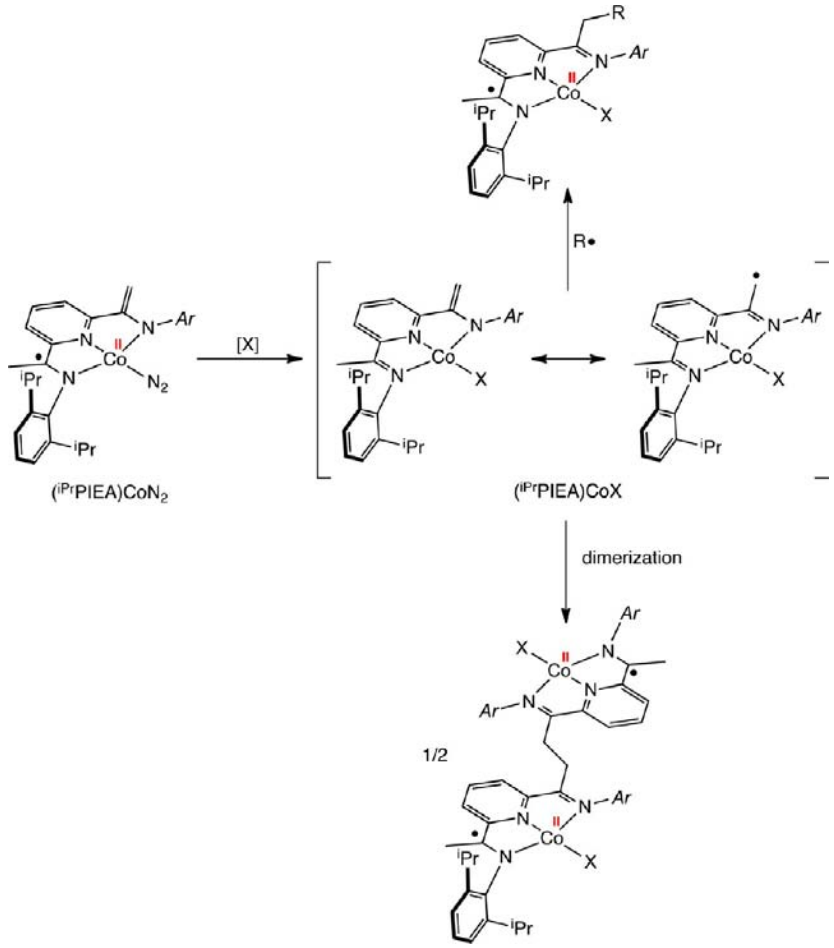

Support for the pathway shown in Scheme 3 was provided by broken-symmetry DFT calculations on the putative (^{iPr}PIEA)-CoCl intermediate (Figure 11). Geometry optimization was performed using the crystallographic data from (^{iPr}PIEA)CoN_2 and replacing the dinitrogen ligand with chloride. The calculations, assuming an S = 1/2 ground state, converged to a UKS solution with a SOMO that is primarily cobalt centered with a minor contribution from the enamide carbon. Presented in Figure 11 is the spin density plot highlighting the metal- and enamide-centered spins likely responsible for C−C bond formation. The calculated bond distances are also significantly different from (^{iPr}PIEA)CoN_2 and are consistent with a neutral α-iminopyridine fragment (Table 4). On the basis of these results, the oxidation is a ligand-based process, and the electronic structure of (^{iPr}PIEA)CoCl is best described as a low-spin Co(II) center with two L-type and two X-type ligands.

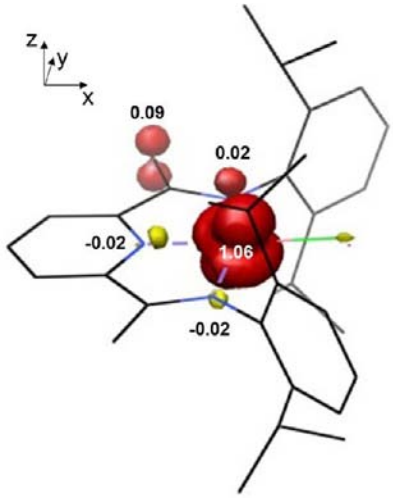

Figure 11. Spin density plot for (^{iPr}PIEA)CoCl obtained from Mulliken population analysis (red, positive spin density; yellow, negative spin density).

Reduction of Coupled-(^{iPr}PDI)CoCl: Cleavage of the C−C Bond. The reversibility of the C−C bond forming reaction was also explored. We reasoned that reduction of Coupled-(^{iPr}PDI)CoX compounds would provide the necessary electronic structure requirements to support regeneration of the enamide ligand. Stirring a toluene solution of Coupled-(^{iPr}PDI)CoCl with two equivalents of $NaBEt_3H$ for three days at ambient temperature resulted in complete conversion to (^{iPr}PIEA)CoN_2 as judged by IR and NMR spectroscopies (eq 6).

Analysis of aliquots of the reaction mixture by infrared and EPR spectroscopy revealed the intermediacy of a second cobalt dinitrogen complex. A diagnostic N−N band was observed at 2090 cm^{-1}, consistent with the presence of a terminal dinitrogen ligand. The X-band EPR spectrum (Figure 12) recorded in a toluene solution at 23 °C exhibited an isotropic signal with g_{iso} = 2.00 (A_{iso} = 8.1 G), reminiscent of the spectrum

dx.doi.org/10.1021/ic400352r | Inorg. Chem. 2013, 52, 5403−5417

Table 4. Comparison of the Experimental Metrical Parameters for (^{iPr}PIEA)CoN_2 to the Computed Values for (^{iPr}PIEA)CoCl[a]

	(^{iPr}PIEA)CoN_2	(^{iPr}PIEA)CoCl
Co(1)−N(1)	1.8679(17)	2.020
Co(1)−N(2)	1.8216(16)	1.862
Co(1)−N(3)	1.8586(17)	1.887
Co(1)−N(4)	1.8176(19)	
N(1)−C(2)	1.364(2)	1.303
N(2)−C(3)	1.372(2)	1.352
N(2)−C(7)	1.364(3)	1.345
N(3)−C(8)	1.373(3)	1.384
C(1)−C(2)	1.475(3)	1.501
C(2)−C(3)	1.429(3)	1.470
C(7)−C(8)	1.468(2)	1.479
C(8)−C(9)	1.400(3)	1.363
N(4)−N(5)	1.110(3)	
N(1)−Co(1)−N(2)	82.27(7)	80.68
N(1)−Co(1)−N(3)	165.08(7)	163.17
N(1)−Co(1)−N(4)	97.48(8)	
N(2)−Co(1)−N(3)	82.83(7)	82.95
N(2)−Co(1)−N(4)	179.34(8)	
N(3)−Co(1)−N(4)	97.40(8)	
Co(1)−N(4)−N(5)	179.2(2)	

[a]Bond distances are reported in Å and bond angles in deg.

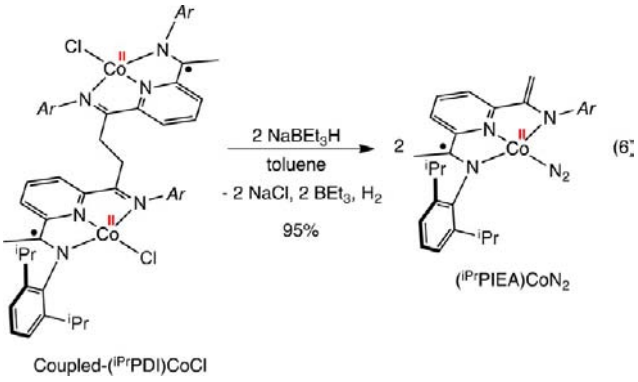

reported for (^{iPr}PDI)CoN_2.[32] It is proposed that this intermediate is Coupled-(^{iPr}PDI)CoN_2, which eventually converts to (^{iPr}PIEA)CoN_2 over longer reaction times. Because of the spectral similarity between the putative Coupled-(^{iPr}PDI)CoN_2 and (^{iPr}PDI)CoN_2, an additional control experiment was conducted. Heating separate benzene-d_6 solutions of (^{iPr}PDI)CoN_2 and (^{iPr}PIEA)CoN_2 to 65 °C for three days produced no change. Because the intermediate formed in the C−C cleavage reaction involving Coupled-(^{iPr}PDI)CoCl is transient under the same conditions, it therefore must be a distinct chemical entity, supporting its formulation as Coupled-(^{iPr}PDI)CoN_2.

CONCLUDING REMARKS

The electronic structure of the pyridine(imine) enamide cobalt dinitrogen complex, (^{iPr}PIEA)CoN_2, is best described as low spin Co(II) antiferromagnetically coupled to a chelate-centered radical. Displacement of the N_2 ligand by halides, pseudohalides, or nitric oxide likely forms (^{iPr}PIEA)CoX, which DFT calculations have shown exhibits radical character on the enamide carbon. In the presence of a long-lived alkyl radical

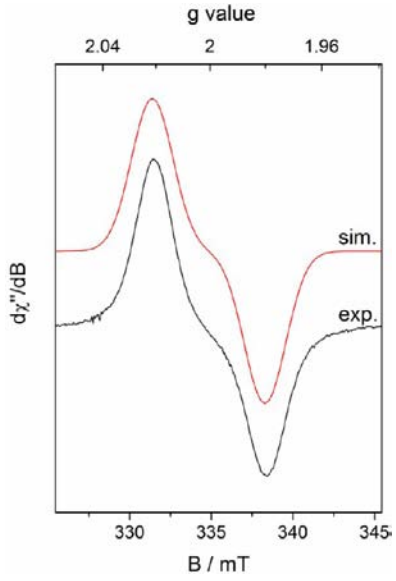

Figure 12. Toluene solution EPR spectrum of the reduction of coupled-(^{iPr}PDI)CoCl with $NaBEt_3H$ recorded at 23 °C (microwave frequency 9.37 GHz, power 2.0 mW, modulation 0.1 mT/100kHz).

such as allyl or benzyl, C−C bond formation results and forms a monomeric, C_s symmetric bis(imino)pyridine cobalt halide complex where the enamide backbone has been homologated. In the absence of such a trapping agent, dimerization occurs to form a bimetallic bis(imino)pyridine cobalt derivative. The C−C bond formation in such compounds is reversible as reduction with $NaBEt_3H$ regenerates (^{iPr}PIEA)CoN_2. In summary, these studies show that the established redox-activity of this chelate class also enables ligand-based reactivity that may ultimately be exploited in catalysis or small molecule activation schemes.

EXPERIMENTAL SECTION

General Considerations. All air- and moisture-sensitive manipulations were carried out using standard vacuum line, Schlenk, and cannula techniques or in an MBraun inert atmosphere drybox containing an atmosphere of purified nitrogen. The MBraun drybox was equipped with a cold well designed for freezing samples in liquid nitrogen. Solvents for air- and moisture-sensitive manipulations were initially dried and deoxygenated using literature procedures.[69]

Nitric oxide gas was purchased from Aldrich. Benzene-d_6 was purchased from Cambridge Isotope Laboratories and distilled from sodium metal under an atmosphere of argon and stored over 4 Å molecular sieves. Ph_3CCl and Ph_2S_2 were purchased from Alfa Aesar and dried under high vacuum conditions. Benzylchloride (Acros Organics) and allylbromide (TCI America) were dried over calcium hydride. The cobalt complex (^{iPr}PDI)CoN_2 was prepared according to the reported literature method.[32]

^{1}H and ^{13}C NMR spectra were recorded at 23 °C on Bruker 300 and 500 and Inova 400 spectrometers operating at 299.763, 500.62, and 399.780 MHz, respectively. All chemical shifts are reported relative to $SiMe_4$ using ^{1}H (residual) chemical shifts of the solvent as a secondary standard. Infrared spectra were collected on a Thermo Nicolet spectrometer. Elemental analyses were performed at Robertson Microlit Laboratories, Inc., in Ledgewood, NJ.

Single crystals suitable for X-ray diffraction were coated with polyisobutylene oil in a drybox, transferred to a nylon loop, and then quickly transferred to the goniometer head of a Bruker APEX2 DUO diffractometer equipped with molybdenum and copper X-ray tubes (λ = 0.71073 Å and 1.54184 Å, respectively). Preliminary data revealed the crystal system. Data collection was optimized for completeness and redundancy using the Bruker COSMO software suite. The space group was identified, and the data were processed using the Bruker SAINT+

dx.doi.org/10.1021/ic400352r | Inorg. Chem. 2013, 52, 5403−5417

program and corrected for absorption using SADABS. The structures were solved using direct methods (SHELXS) completed by subsequent Fourier synthesis and refined by full-matrix least-squares procedures.

The X-band EPR derivative spectrum was recorded on a Bruker EMX Plus Standard Resonator spectrometer (resonance frequency = 9.85 GHz) equipped with the Bruker standard cavity (E4119001) and a helium flow cryostat (Oxford Instruments ITC 503S). The spectrum was simulated with the program GFIT (by Eckhard Bill) for the calculation of powder spectra with effective g values and anisotropic line widths (Gaussian line shapes were used).

Quantum Chemical Calculations. All DFT calculations were performed with the ORCA program package as described previously.[51] The geometry optimizations of the complexes and single-point calculations on the optimized geometries were carried out at the B3LYP level of DFT. This hybrid functional often gives better results for transition metal compounds than pure gradient-corrected functionals, especially with regard to metal−ligand covalency. The all-electron Gaussian basis sets were those developed by the Ahlrichs group. Triple-ζ quality basis sets def2-TZVP with one set of polarization functions on cobalt and on the atoms directly coordinated to the metal center were used. For the carbon and hydrogen atoms, slightly smaller polarized split-valence def2-SV(P) basis sets were used that were of double-ζ quality in the valence region and contained a polarizing set of d functions on the non-hydrogen atoms. Auxiliary basis sets were chosen to match the orbital basis. The RIJCOSX approximation was used to accelerate the calculations. Canonical and corresponding orbitals, as well as spin density plots, were generated with the program Molekel.[70]

Preparation of (^{iPr}PIEA)CoN$_2$. A 100 mL round-bottom flask was charged with 0.207 g (0.359 mmol) of (^{iPr}PDI)CoCl, approximately 50 mL of tetrahydrofuran, and a stir bar. NaO^{t}Bu (0.035 g, 0.364 mmol) was added, and the reaction was stirred for three days, during which time a gradual color change to red was observed. The volatiles were removed, and the solid was extracted into a 3:1 diethyl ether−toluene mixture. The resulting dark green solution was filtered through Celite. The solution was concentrated and cooled to −35 °C, yielding 0.130 g (63%) of dark brown powder identified as (^{iPr}PIEA)CoN$_2$. Analysis for C33H42N5Co, Calcd.: C, 69.82; H, 7.46; N, 12.34. Found: C, 69.84; H, 7.59; N, 11.98. ^{1}H NMR (benzene-d_6): δ −0.71 (s, 3H, N=CCH_3), 0.89 (d, 6.9 Hz, 6H, CH(CH_3)$_2$), 1.22 (d, 6.6 Hz, 6H, CH(CH_3)$_2$), 1.23 (d, 6.6 Hz, 6H, CH(CH_3)$_2$), 1.39 (d, 6.9 Hz, 6H, CH(CH_3)$_2$), 2.70 (septet, 6.9 Hz, 2H, CH(CH$_3$)$_2$), 3.25 (septet, 6.6 Hz, 2H, CH(CH$_3$)$_2$), 4.05 (s, 1H, NC=CH_2), 4.73 (s, 1H, NC=CH_2), 7.08−7.22 (m, 6H, m-Ar and p-Ar), 7.24 (t, 7.7 Hz, 1H, p-py), 7.38 (d, 7.7 Hz, 1H, m-py), 8.30 (d, 7.7 Hz, 1H, m-py). {^{1}H}^{13}C NMR (benzene-d_6): δ 19.84(C(CH$_3$)), 24.03 (CH(CH_3)$_2$), 24.69 (CH-(CH_3)$_2$), 24.72 (CH(CH_3)$_2$), 25.89(CH(CH_3)$_2$), 28.16 (CH(CH$_3$)$_2$), 29.03 (CH(CH$_3$)$_2$), 90.33 (C=CH$_2$), 111.30 (m-py), 117.94 (m-py), 123.74 (m- or p-Ar), 123.87 (m- or p-Ar), 123.99 (m- or p-Ar), 126.00 (m- or p-Ar), 132.81 (p-py), 139.91, 141.42, 142.06, 145.57, 151.43, 159.54, 161.43, 164.67. IR (toluene): υ_{NN} = 2145 cm^{-1}. IR (KBr): υ_{NN} = 2148 cm^{-1}, υ_{CC} = 1583 cm^{-1}.

Preparation of Coupled-(^{iPr}PDI)CoCl. A 20 mL scintillation vial was charged with 53 mg (0.093 mmol) of (^{iPr}PIEA)CoN$_2$ and approximately 10 mL of toluene. In a second vial, 26 mg (0.093 mmol, 1.0 equiv) of Ph$_3$CCl was dissolved in 5 mL of toluene, and the resulting clear solution was added dropwise to the first vial. A color change to dark pink was observed by the end of the addition. The reaction was stirred at room temperature for 30 min to ensure complete conversion of the starting materials to products. The solution was concentrated to approximately 0.5 mL, and approximately 5 mL of pentane was added. Recrystallization at −35 °C overnight yielded 46 mg (0.040 mmol, 86%) of dark pink crystals identified as Coupled-(^{iPr}PDI)CoCl. Single crystals suitable for X-ray diffraction were prepared in THF/pentane. Analysis for C$_{66}$H$_{84}$Cl$_2$Co$_2$N$_6$, Calcd.: C, 68.92; H, 7.36; N, 7.31. Found: C, 69.20; H, 7.70; N, 7.08. ^{1}H NMR (benzene-d_6): δ 0.34 (s, 6H, N=C(CH_3)), 1.00 (d, 6.8 Hz, 12H, CH(CH_3)$_2$), 1.12 (d, 6.8 Hz, 12H, CH(CH_3)$_2$), 1.16 (d, 6.8 Hz, 12H, CH(CH_3)$_2$), 1.26 (d, 6.8 Hz, 12H, CH(CH_3)$_2$), 2.58 (s, 4H, N=C(CH_2)), 3.34 (septet, 6.8 Hz, 4H, CH(CH$_3$)$_2$), 3.46 (septet, 6.8 Hz, 4H, CH(CH$_3$)$_2$), 6.65 (d, 7.7 Hz, 2H, m-py), 7.09 (d, 7.7 Hz, 2H, m-py), 7.23 (d, 7.8 Hz, 4H, m-Ar), 7.38 (t, 7.8 Hz, 2H, p-Ar), 7.41 (d, 7.9 Hz, 4H, m-Ar), 7.59 (t, 7.9 Hz, 2H, p-Ar), 9.67 (pseudo t, 7.7 Hz, 2H, p-py). {^{1}H} ^{13}C NMR (benzene-d_6): δ 20.66 (N=C(CH$_2$)), 21.23 (N=C(CH$_3$)), 23.63 (CH(CH$_3$)$_2$), 23.78 (CH(CH$_3$)$_2$), 24.22 (CH(CH$_3$)$_2$), 25.17 (CH(CH$_3$)$_2$), 29.04 (CH(CH$_3$)$_2$), 29.28 (CH(CH$_3$)$_2$), 116.62 (p-py), 123.84 (m-Ar), 124.39 (m-Ar), 125.21 (m-py), 126.20 (m-py), 127.13 (p-Ar), 127.17 (p-Ar), 140.85 (o-Ar), 141.21 (o-Ar), 150.02 (i-Ar), 151.55 (o-py), 151.96 (i-Ar), 154.45 (o-py), 164.40 (N=C(CH$_2$)), 169.77 (N=C(CH$_3$)).

Preparation of Benzyl-(^{iPr}PDI)CoCl. A 20 mL scintillation vial was charged with 10 mg (0.018 mmol) of (^{iPr}PIEA)CoN$_2$ and approximately 0.7 mL of benzene-d_6. Via microsyringe, 2 μL (0.017 mmol, 1 equiv) of benzyl chloride was added, and the reaction was stirred at room temperature for one hour. A color change from dark green to dark pink was observed. The reaction was filtered into a J. Young NMR tube and analyzed by NMR spectroscopy, establishing a 3:1 mixture of Benzyl-(^{iPr}PDI)CoCl and Coupled-(^{iPr}PDI)CoCl. ^{1}H NMR (benzene-d_6): δ 0.19 (s, 3H, N=C(CH_3)), 1.06 (d, 7.1 Hz, 6H, CH(CH_3)$_2$), 1.12 (d, 6.7 Hz, 6H, CH(CH_3)$_2$), 1.21 (d, 6.7 Hz, 6H, CH(CH_3)$_2$), 1.24 (d, 7.2 Hz, 6H, CH(CH_3)$_2$), 2.19 (t, 7.3 Hz, 2H, N=C(CH_2CH$_2$Ph)), 3.14 (t, 7.3 Hz, 2H, N=C(CH$_2$CH_2Ph)), 3.36 (septet, 7.1 Hz, 2H, CH(CH$_3$)$_2$), 3.42 (septet, 6.7 Hz, 2H, CH(CH$_3$)$_2$), 7.00 (d, 8.0 Hz, 1H, m-py), 7.01 (t, 7.4 Hz, 1H, p-Ph), 7.06 (d, 8.0 Hz, 1H, m-py), 7.08 (d, 7.1 Hz, 2H, o-Ph), 7.22 (t, 7.7 Hz, 1H, p-Ar), 7.26 (d, 7.7 Hz, 2H, m-Ar), 7.33 (d, 7.7 Hz, 2H, m-Ar), 7.41 (dd, 7.4 Hz, 7.1 Hz, 2H, m-Ph), 7.47 (t, 7.7 Hz, 1H, p-Ar), 9.55 (pseudo t, 8.0 Hz, 1H, p-py). {^{1}H} ^{13}C NMR (benzene-d_6): δ 21.38 (N=C(CH$_3$)), 23.43 (N=C(CH$_2$CH$_2$Ph)), 23.83 (CH(CH$_3$)$_2$), 23.93 (CH(CH$_3$)$_2$), 24.14 (CH(CH$_3$)$_2$), 24.71 (CH(CH$_3$)$_2$), 29.08 (CH(CH$_3$)$_2$), 29.24 (CH(CH$_3$)$_2$), 37.68 (N=C(CH$_2$CH$_2$Ph)), 115.47 (p-py), 123.96 (m-Ar), 125.37 (m-py), 126.13 (m-py), 126.82 (p-Ph), 127.13 (p-Ar), 127.29 (p-Ar), 128.35 (o-Ph), 128.81 (m-Ar), 129.34 (m-Ph), 139.93 (i-Ph), 140.80 (o-Ar), 140.85 (o-Ar), 150.60 (i-Ar), 151.02 (i-Ar), 152.17 (o-py), 153.56 (o-py), 168.34 (N=C(CH$_3$)), 169.20 (N=C(CH$_2$CH$_2$Ph)).

Preparation of Coupled-(^{iPr}PDI)CoBr. A thick-walled glass vessel was charged with 32 mg (0.056 mmol) of (^{iPr}PIEA)CoN$_2$ and approximately 10 mL of toluene. The reaction vessel was degassed, and 0.056 mmol (33 Torr, 31.6 mL; 1.0 equiv) of allylbromide was admitted using a calibrated gas bulb. The solution was thawed to room temperature and stirred for an hour. A color change to dark pink was observed. The solution was concentrated to approximately 0.5 mL, and about 3 mL of pentane was added. Recrystallization at −35 °C overnight yielded 25 mg (0.020 mmol, 72%) of dark pink crystals identified as Coupled-(^{iPr}PDI)CoBr. Single crystals suitable for X-ray diffraction were prepared in benzene. Analysis for C$_{66}$H$_{84}$Br$_2$Co$_2$N$_6$, Calcd.: C, 63.97; H, 6.83; N, 6.78. Found: C, 63.95; H, 6.91; N, 6.48. ^{1}H NMR (benzene-d_6): δ 0.21 (s, 6H, N=C(CH_3)), 1.06 (d, 6.6 Hz, 12H, CH(CH_3)$_2$), 1.12 (d, 6.4 Hz, 12H, CH(CH_3)$_2$), 1.24 (d, 6.4 Hz, 12H, CH(CH_3)$_2$), 1.27 (d, 6.6 Hz, 12H, CH(CH_3)$_2$), 2.51 (s, 4H, N=C(CH_2)), 3.39 (septet, 6.6 Hz, 4H, CH(CH$_3$)$_2$), 3.52 (septet, 6.4 Hz, 4H, CH(CH$_3$)$_2$), 6.63 (d, 7.4 Hz, 2H, m-py), 7.08 (d, 7.4 Hz, 2H, m-py), 7.27 (d, 7.7 Hz, 4H, m-Ar), 7.42 (t, 7.7 Hz, 2H, p-Ar), 7.47 (d, 7.6 Hz, 4H, m-Ar), 7.67 (t, 7.6 Hz, 2H, p-Ar), 9.90 (pseudo t, 7.4 Hz, 2H, p-py). {^{1}H} ^{13}C NMR (benzene-d_6): δ 20.48 (N=C(CH$_2$)), 21.99 (N=C(CH$_3$)), 23.66 (CH(CH$_3$)$_2$), 23.91 (CH(CH$_3$)$_2$), 24.41 (CH(CH$_3$)$_2$), 25.12 (CH(CH$_3$)$_2$), 29.04 (CH(CH$_3$)$_2$), 29.26 (CH-(CH$_3$)$_2$), 116.83 (p-py), 123.92 (m-Ar), 124.55 (m-Ar), 125.21 (m-py), 126.34 (m-py), 127.31 (p-Ar), 140.64 (o-Ar), 140.91 (o-Ar), 151.29 (i-Ar), 151.42 (o-py), 153.32 (i-Ar), 154.54 (o-py), 165.10 (N=C(CH$_2$)), 170.74 (N=C(CH$_3$)).

Preparation of Allyl-(^{iPr}PDI)CoBr. A J. Young tube was charged with 14 mg (0.025 mmol) of (^{iPr}PIEA)CoN$_2$ and approximately 0.7 mL of benzene-d_6. The tube was degassed and 0.025 mmol (35 Torr, 13.1 mL; 1.0 equiv) of allylbromide was admitted using a calibrated gas bulb. The solution was thawed and allowed to stand at room temperature for an hour. A color change to dark pink was observed. The volatiles were distilled into a second tube and analyzed by NMR

dx.doi.org/10.1021/ic400352r | Inorg. Chem. 2013, 52, 5403−5417

spectroscopy and established formation of 1,5-hexadiene. The remaining residue in the reaction tube was determined to be an approximately 1:3 mixture of Coupled-(^{iPr}PDI)CoBr and Allyl-(^{iPr}PDI)CoBr. ^{1}H NMR (benzene-d_6): δ 0.01 (s, 3H, N=C(CH_3)), 1.10−1.26 (overlaps with other resonances; d, 24H, CH(CH_3)$_2$), 1.80 (t, 8.2 Hz, 2H, N=C(CH_2-allyl)), 2.56 (m, 8.2 Hz, 6.7 Hz, 2H, CH_2CH=CH$_2$)), 2.96 (septet, 7.2 Hz, 2H, CH(CH$_3$)$_2$), 3.38 (septet, 7.2 Hz, 2H, CH(CH$_3$)$_2$), 4.83 (d, 8.7 Hz, 1H, CH$_2$CH=C(H)H_{cis}), 4.92 (d, 17.1 Hz, 1H, CH$_2$CH=C(H)H_{trans}), 5.52 (m, 17.1 Hz, 8.7 Hz, 6.7 Hz, 1H CH$_2$CH=CH$_2$), 6.94 (d, 7.6 Hz, 1H, m-py), 6.98 (d, 7.8 Hz, 1H, m-py), 7.18−7.30 (overlaps with other resonances, 6H, Ar−H), 9.76 (dd, 7.8 Hz, 7.6 Hz, 1H, p-py). {^{1}H} ^{13}C NMR (benzene-d_6): δ 21.29 (CH$_2$CH=CH$_2$), 21.89 (N=C(CH$_3$)), 24.18 (CH(CH$_3$)$_2$), 24.26 (CH(CH$_3$)$_2$), 24.31 (CH(CH$_3$)$_2$), 24.41 (CH-(CH$_3$)$_2$), 29.08 (CH(CH$_3$)$_2$), 29.11 (CH(CH$_3$)$_2$), 35.48 (N=C(CH$_2$-allyl), 115.65 (CH$_2$CH=CH$_2$), 115.45 (p-py), 123.88 (m-Ar), 126.14 (m-py), 127.04 (m-py), 127.29 (p-Ar), 136.05 (CH$_2$CH=CH$_2$), 140.53 (o-Ar), 140.60 (o-Ar), 151.21 (i-Ar), 151.94 (o-py), 152.05 (i-Ar), 153.36 (o-py), 169.00 (N=C(CH$_3$)), 170.34 (N=C(CH$_2$-allyl)).

Preparation of Coupled-(^{iPr}PDI)CoSPh. A 20 mL scintillation vial was charged with 60 mg (0.11 mmol) of (^{iPr}PIEA)CoN$_2$ and approximately 10 mL of toluene. In a second vial, 12 mg (0.055 mmol, 0.5 equiv) of Ph$_2$S$_2$ was dissolved in 1 mL of toluene. The resulting solution was added to the first vial dropwise, and the reaction was stirred for an hour. A color change from dark green to dark pink was observed. The solution was concentrated to approximately 0.5 mL, and about 3 mL of pentane was added. Recrystallization at −35 °C overnight yielded 50 mg (0.039 mmol, 72%) of dark pink crystals identified as Coupled-(^{iPr}PDI)CoSPh. Single crystals suitable for X-ray diffraction were obtained from benzene. Analysis for C$_{78}$H$_{94}$Co$_2$N$_6$S$_2$, Calcd.: C, 72.20; H, 7.30; N, 6.48. Found: C, 74.86; H, 6.92; N, 6.54. ^{1}H NMR (benzene-d_6): δ 0.36 (s, 6H, N=C(CH_3)), 1.04 (d, 6.6 Hz, 12H, CH(CH_3)$_2$), 1.10 (d, 6.7 Hz, 12H, CH(CH_3)$_2$), 1.14 (d, 6.7 Hz, 12H, CH(CH_3)$_2$), 1.32 (d, 6.6 Hz, 12H, CH(CH_3)$_2$), 2.62 (s, 4H, N=C(CH_2)), 3.28 (septet, 6.7 Hz, 4H, CH(CH$_3$)$_2$), 3.38 (septet, 6.6 Hz, 4H, CH(CH$_3$)$_2$), 6.68 (t, 7.4 Hz, 4H, m-SPh), 6.85 (d, 7.4 Hz, 4H, o-SPh), 6.89 (t, 7.4 Hz, 2H, p-SPh), 6.90 (d, 7.6 Hz, 2H, m-py), 6.99 (d, 7.7 Hz, 4H, m-Ar), 7.16 (t, 7.7 Hz, 2H, p-Ar), 7.29 (d, 7.8 Hz, 4H, m-Ar), 7.43 (d, 7.6 Hz, 2H, m-py), 7.53 (t, 7.8 Hz, 2H, p-Ar), 9.28 (pseudo t, 7.6 Hz, 2H, p-py). {^{1}H} ^{13}C NMR (benzene-d_6): δ 22.61 (N=C(CH$_2$)), 22.00 (N=C(CH$_3$)), 23.80 (CH(CH$_3$)$_2$), 23.88 (CH(CH$_3$)$_2$), 24.47 (CH(CH$_3$)$_2$), 25.63 (CH(CH$_3$)$_2$), 28.73 (CH-(CH$_3$)$_2$), 29.10 (CH(CH$_3$)$_2$), 117.37 (p-py), 122.72 (p-SPh), 123.87 (m-Ar), 123.77 (m-py), 124.47 (m-Ar), 124.90 (m-py), 127.01 (p-Ar), 127.11 (p-Ar), 127.69 (m-SPh), 135.62 (o-SPh), 140.52 (o-Ar), 141.47 (o-Ar), 142.72 (i-SPh), 149.87 (o-py), 150.18 (i-Ar), 151.05 (i-Ar), 151.72 (o-py), 163.12 (N=C(CH$_2$)), 166.98 (N=C(CH$_3$)).

Preparation of Coupled-(^{iPr}PDI)CoNO. A thick-walled glass vessel was charged with 0.126 g (0.222 mmol) of (^{iPr}PIEA)CoN$_2$ and approximately 10 mL of toluene. A dark teal solution formed, and the vessel was submerged in liquid nitrogen and degassed. The solution was thawed to room temperature and opened to a calibrated gas bulb containing 0.21 mmol (39 Torr, 100.1 mL; 0.95 equiv) of NO gas. A color change to fuchsia was observed. The resulting solution was stirred at room temperature for 1 h to ensure complete conversion to the cobalt nitrosyl complex. The solution was then concentrated to approximately 1 mL followed by the addition of about 3 mL of pentane. Recrystallization at −35 °C overnight yielded 0.121 g (0.106 mmol, 96%) of dark pink crystals identified as Coupled-(^{iPr}PDI)-CoNO. Single crystals suitable for X-ray diffraction were also prepared in toluene/pentane. Analysis for C$_{66}$H$_{84}$Co$_2$N$_4$O$_2$, Calcd.: C, 69.58; H, 7.43; N, 9.84. Found: C, 69.29; H, 7.41; N, 9.41. ^{1}H NMR (benzene-d_6): δ 1.09 (d, 6.6 Hz, 12H, CH(CH_3)$_2$), 1.10 (d, 6.6 Hz, 12H, CH(CH_3)$_2$), 1.17 (d, 6.6 Hz, 12H, CH(CH_3)$_2$), 1.18 (d, 6.6 Hz, 12H, CH(CH_3)$_2$), 2.06 (s, 6H, N=C(CH_3)), 3.20 (septet, 6.6 Hz, 4H, CH(CH$_3$)$_2$), 3.21 (septet, 6.6 Hz, 4H, CH(CH$_3$)$_2$), 3.56 (s, 4H, N=C(CH_2)), 6.97 (d, 7.8 Hz, 2H, m-py), 7.10 (dd, 7.8 Hz, 7.3 Hz, 2H, p-py), 7.16 (t, 7.6 Hz, 2H, p-Ar), 7.18 (d, 7.6 Hz, 4H, m-Ar), 7.21 (t, 7.6 Hz, 2H, p-Ar), 7.29 (d, 7.6 Hz, 4H, m-Ar), 7.46 (d, 7.3 Hz, 2H, m-py). {^{1}H}^{13}C NMR (benzene-d_6): δ 17.11 (N=C(CH$_3$)), 23.21 (CH(CH$_3$)$_2$), 24.32 (CH(CH$_3$)$_2$), 24.42 (CH(CH$_3$)$_2$), 25.47 (CH-(CH$_3$)$_2$), 28.18 (CH(CH$_3$)$_2$), 28.51 (CH(CH$_3$)$_2$), 28.84 (N=C(CH$_2$)), 119.90 (m-py), 121.16 (m-py), 122.70 (p-py), 123.66 (m-Ar), 124.09 (m-Ar), 126.70 (p-Ar), 126.78 (p-Ar), 140.79 (o-Ar), 141.22 (o-py), 141.52 (o-Ar), 142.12 (o-py), 149.17 (i-Ar), 149.44 (i-Ar), 155.66 (N=C(CH$_2$)), 157.43 (N=C(CH$_3$)). IR (benzene-d_6): υ_{NO} = 1712 cm^{-1}.

Reduction of Coupled-(^{iPr}PDI)CoCl with NaBEt$_3$H. A 20 mL scintillation vial was charged with 53 mg (0.046 mmol) of Coupled-(^{iPr}PDI)CoCl and approximately 5 mL of toluene. The solution was cooled and 0.090 mL of a 1.0 M solution (0.090 mmol, 1.95 equiv) of NaBEt$_3$H in toluene was added. The reaction was stirred at room temperature for 3 days, after which time a color change to dark green was observed. Analysis of the resulting mixture by IR and NMR spectroscopies showed complete conversion of Coupled-(^{iPr}PDI)CoCl to (^{iPr}PIEA)CoN$_2$.

Preparation of (^{iPr}PDI)CoNO. This compound was prepared in a manner similar to the synthesis of Coupled-(^{iPr}PDI)CoNO using 0.139 g (0.244 mmol) of (^{iPr}PDI)CoN$_2$ and 0.23 mmol (43 Torr, 100.1 mL; 0.95 equiv) of NO gas. Recrystallization at −35 °C overnight yielded 0.120 g (86%) of dark pink crystals identified as (^{iPr}PDI)CoNO. Single crystals suitable for X-ray diffraction were prepared in toluene/pentane. Analysis for C$_{33}$H$_{43}$CoN$_4$O, Calcd.: C, 69.46; H, 7.60; N, 9.82. Found: C, 69.26; H, 7.43; N, 9.69. ^{1}H NMR (benzene-d_6): δ 1.08 (d, 6.9 Hz, 12H, CH(CH_3)$_2$), 1.15 (d, 6.9 Hz, 12H, CH(CH_3)$_2$), 2.05 (s, 6H, N=C(CH_3)), 3.18 (septet, 6.9 Hz, 4H, CH(CH$_3$)$_2$), 6.98 (t, 7.7 Hz, 1H, p-py), 7.16 (d, 7.6 Hz, 4H, m-Ar), 7.21 (t, 7.6 Hz, 2H, p-Ar), 7.45 (d, 7.7 Hz, 2H, m-py). {^{1}H} ^{13}C NMR (benzene-d_6): δ 17.24 (N=C(CH$_3$)), 24.13 (CH(CH$_3$)$_2$), 24.45 (CH(CH$_3$)$_2$), 28.59 (CH(CH$_3$)$_2$), 120.58 (m-py or p-Ar), 121.68 (p-py), 123.90 (m-Ar), 126.99 (m-py or p-Ar), 141.11 (i-Ar or o-Ar), 141.72 (i-Ar or o-Ar), 149.73 (o-py), 155.72 (N=C(CH$_3$)). IR (benzene-d_6): υ_{NO} = 1712 cm^{-1}. IR (KBr): υ_{NO} = 1709 cm^{-1}.

■ ASSOCIATED CONTENT

Ⓢ Supporting Information

Crystallographic details for (^{iPr}PIEA)CoN$_2$, Coupled-(^{iPr}PDI)-CoCl, Coupled-(^{iPr}PDI)CoBr, Coupled-(^{iPr}PDI)CoSPh, Coupled-(^{iPr}PDI)CoNO, and (^{iPr}PDI)CoNO in cif format. This material can be downloaded, free of charge, via the Internet at http://pubs.acs.org.

■ AUTHOR INFORMATION

Corresponding Author

*E-mail: pchirik@princeton.edu.

Notes

The authors declare no competing financial interest.

■ ACKNOWLEDGMENTS

We thank the U.S. National Science Foundation and the Deutsche Forschungsgemeinschaft for a Cooperative Activities in Chemistry between U.S. and German Investigators grant (CHE-1026084). C.M. is grateful to the Alexander von Humboldt Foundation for a postdoctoral research fellowship. S.P.S. thanks the Natural Sciences and Engineering Research Council of Canada for a predoctoral fellowship (PGS-D). Z.R.T. thanks the U.S.−U.K. Fulbright Commission and AstraZeneca for a fellowship. We also thank Prof. Amanda Bowman for initial studies in the preparation and characterization of (^{iPr}PDI)CoNO.

■ REFERENCES

(1) Chirik, P. J. *Inorg. Chem.* **2011**, *50*, 9737.
(2) Kaim, W. *Eur. J. Inorg. Chem.* **2012**, 343.
(3) (a) Stubbe, J.; Van der Donk, W. A. *Chem. Rev.* **1998**, *98*, 706. (b) Jazdewski, B. A.; Tolman, W. B. *Coord. Chem. Rev.* **2000**, *200*−*202*,

633. (c) Lewis, E. A.; Tolman, W. B. *Chem. Rev.* **2004**, *104*, 1047. (d) Kaim, W.; Schwederski, B. *Coord. Chem. Rev.* **2010**, *254*, 1580.
(4) Rittle, J.; Green, M. T. *Science* **2010**, *330*, 933.
(5) Chaudhuri, P.; Wieghardt, K. *Prog. Inorg. Chem.* **2001**, *50*, 151.
(6) Stanciu, C.; Jones, M. E.; Fanwick, P. E.; Abu-Omar, M. *J. Am. Chem. Soc.* **2007**, *129*, 12400.
(7) (a) Heyduk, A. F.; Zarkesh, R. A.; Nguyen, A. I. *Inorg. Chem.* **2011**, *50*, 9849. (b) Nguyen, N.; Zarkesh, R. A.; Lacy, D. C.; Thorson, M. K.; Heyduk, A. F. *Chem. Sci.* **2011**, *2*, 166. (c) Zarkesh, R. A.; Ziller, J. W.; Heyduk, A. F. *Angew. Chem., Int. Ed.* **2008**, *47*, 4715.
(8) King, E. R.; Hennessy, E. T.; Betley, T. A. *J. Am. Chem. Soc.* **2011**, *133*, 4917.
(9) Chirik, P. J.; Wieghardt, K. *Science* **2010**, *327*, 794.
(10) Blanchard, S.; Derat, E.; Desage-El Murr, M.; Fensterbank, Malacria, M.; Mouriès-Mansuy, V. *Eur. J. Inorg. Chem.* **2012**, 376.
(11) van der Vlugt, J. I. *Eur. J. Inorg. Chem.* **2012**, 363.
(12) Caulton, K. G. *Eur. J. Inorg. Chem.* **2012**, 435.
(13) For selected examples of strategies employing redox-activity at reactive carbon-based ligands for C−C bond constructions, see: (a) Schauer, P. A.; Low, P. J. *Eur. J. Inorg. Chem.* **2012**, 390. (b) Berry, J. F. *Dalton Trans.* **2012**, *41*, 700. (c) Lyaskovskyy, V.; de Bruin, B. *ACS Catal.* **2012**, *2*, 270. (d) Lu, H.; Dzik, W. I.; Xu, X.; Wojtas, L.; de Bruin, B.; Zhang, X. P. *J. Am. Chem. Soc.* **2011**, *133*, 8518.
(14) For early examples in ruthenium alkyne chemistry, see: (a) Muller, F.; Dijkhuis, D. I. P.; van Koten, G.; Vrieze, K.; Heijdenrijk, D.; Rotteveel, M. A.; Stam, C. H.; Zoutberg, M. C. *Organometallics* **1989**, *8*, 992. (b) Muller, F.; van Koten, G.; Polm, L. H.; Vrieze, K.; Zoutberg, M. C.; Heijdenrijk, D.; Kragten, E.; Stam, C. H. *Organometallics* **1989**, *8*, 1340.
(15) (a) Jubb, J.; Floriani, C.; Chiesi-Villa, A.; Rizzoli, C. *J. Am. Chem. Soc.* **1992**, *114*, 6571. (b) Piarulli, U.; Solari, E.; Floriani, C.; Chiesi-Villa, A.; Rizzoli, C. *J. Am. Chem. Soc.* **1996**, *118*, 3634. (c) De Angelis, S.; Solari, E.; Floriani, C.; Chiesi-Villa, A.; Rizzoli, C. *J. Am. Chem. Soc.* **1994**, *116*, 5691. (d) De Angelis, S.; Solari, E.; Floriani, C.; Chies-Villa, A.; Rizzoli, C. *J. Am. Chem. Soc.* **1994**, *116*, 5702. (e) Floriani, C.; Floriani-Moro, R. In *The Porphyrin Handbook*; Kadish, K. M., Smith, K. M., Guilard, R., Eds.; Academic Press: San Diego, CA, 2000; Vol. 3, Chapter 25, pp 405−420. (f) Crescenzi, R.; Solari, E.; Floriani, C.; Chiesi-Villa, A.; Rizzoli, C. *J. Am. Chem. Soc.* **1999**, *121*, 1695. (g) Floriani, C. *Chimia* **1996**, *50*, 608. (h) Belanzoni, P.; Rosi, M.; Sgamellotti, A.; Bonomo, L.; Floriani, C. *J. Chem. Soc., Dalton Trans.* **2001**, 1492.
(16) (a) Bachman, J.; Nocera, D. G. *J. Am. Chem. Soc.* **2004**, *126*, 2829. (b) Bachman, J.; Nocera, D. G. *Inorg. Chem.* **2005**, *44*, 6930. (c) Bachman, J.; Nocera, D. G. *J. Am. Chem. Soc.* **2005**, *127*, 4730. (d) Bachmann, J.; Hodgkiss, J. M.; Young, E. R.; Nocera, D. G. *Inorg. Chem.* **2007**, *46*, 607.
(17) Frazier, B. A.; Wolczanski, P. T.; Lobkovsky, E. B.; Cundari, T. R. *J. Am. Chem. Soc.* **2009**, *131*, 3428.
(18) Frazier, B. A.; Wolczanski, P. T.; Keresztes, I.; DeBeer, S.; Lobkovsky, E. B.; Pierpont, A. W.; Cundari, T. R. *Inorg. Chem.* **2012**, *51*, 8177.
(19) Hulley, E. B.; Wolczanski, P. T.; Lobkovsky, E. B. *J. Am. Chem. Soc.* **2011**, *133*, 18058.
(20) Dugan, T. R.; Bill, E.; Macleod, K. C.; Christian, G. J.; Cowley, R. E.; Brennessel, W. W.; Ye, S.; Neese, F.; Holland, P. L. *J. Am. Chem. Soc.* **2012**, *134*, 20352.
(21) (a) Grumbine, S. D.; Chadha, R. K.; Tilley, T. D. *J. Am. Chem. Soc.* **1992**, *114*, 1518. (b) Cohen, B. W.; Polyansky, D. E.; Zong, R.; Zhou, H.; Ouk, T.; Cabelli, D. E.; Thummel, R. P.; Fujita, E. *Inorg. Chem.* **2010**, *49*, 8034.
(22) Duplessis, E. A.; Jelliss, P. A.; Kirkpatrick, C. C.; Minteer, S. D.; Wampler, K. M. *J. Organomet. Chem.* **2006**, *691*, 4660.
(23) (a) Deelman, B.-J.; Stevels, W. M.; Teuben, J. H.; Lakin, M. T.; Spek, A. L. *Organometallics* **1994**, *13*, 3881. (b) Jaroschik, F.; Nief, F.; Le Goff, X.-F.; Ricard, L. *Organometallics* **2007**, *26*, 3552.
(24) Durfee, L. D.; Fanwick, P. E.; Rothwell, I. P.; Folting, K.; Huffman, J. C. *J. Am. Chem. Soc.* **1987**, *109*, 4720.
(25) deBruin, B.; Bill, E.; Bothe, E.; Weyhermüller, T.; Wieghardt, K. *Inorg. Chem.* **2000**, *39*, 2936.
(26) Bart, S. C.; Chlopek, K.; Bill, E.; Bouwkamp, M. W.; Lobkovsky, E.; Neese, F.; Wieghardt, K.; Chirik, P. J. *J. Am. Chem. Soc* **2006**, *128*, 13901.
(27) Knijnenburg, Q.; Gambarotta, S.; Budzelaar, P. H. M. *Dalton Trans.* **2006**, 5442.
(28) Budzelaar, P. H. M.; de Bruin, B.; Gal, A. W.; Wieghardt, K.; van Lenthe, J. H. *Inorg. Chem.* **2001**, *40*, 4649.
(29) Zhu, D.; Thapa, I.; Korobkov, I.; Gambarotta, S.; Budzelaar, P. H. M. *Inorg. Chem.* **2011**, *50*, 9879.
(30) Sugiyama, H.; Aharonian, G.; Gambarotta, S.; Yap, G. P. A.; Budzelaar, P. H. M. *J. Am. Chem. Soc.* **2002**, *124*, 12268.
(31) Scott, J.; Gambarotta, S.; Korobkov, I.; Budzelaar, P. H. M. *J. Am. Chem. Soc.* **2005**, *127*, 13019.
(32) Bowman, A. C.; Milsmann, C.; Atienza, C. C. H.; Lobkovsky, E.; Wieghardt, K.; Chirik, P. J. *J. Am. Chem. Soc.* **2010**, *132*, 1676.
(33) Bouwkamp, M. W.; Lobkovsky, E.; Chirik, P. J. *Inorg. Chem.* **2006**, *45*, 2.
(34) Vidyaratne, I.; Scott, J.; Gambarotta, S.; Budzelaar, P. H. M. *Inorg. Chem.* **2007**, *46*, 7040.
(35) Scott, J.; Gambarotta, S.; Korobkov, I. *Can. J. Chem.* **2005**, *83*, 279.
(36) Scott, J.; Vidyaratne, I.; Korobkov, I.; Gambarotta, S.; Budzelaar, P. H. M. *Inorg. Chem.* **2008**, *47*, 896.
(37) Zhu, D.; Budzelaar, P. H. M. *Organometallics* **2010**, *29*, 5759.
(38) Zhu, D.; Korobkov, I.; Budzelaar, P. H. M. *Organometallics* **2012**, *31*, 3958.
(39) For other examples of bis(imino)pyridine alkylation, see: (a) Reardon, D.; Conan, F.; Gambarotta, S.; Yap, G.; Wang, Q. *J. Am. Chem. Soc.* **1999**, *121*, 9318. (b) Cámpora, J.; Pérez, C. M.; Rodriguez-Delgado, A.; Naz, A. M.; Palma, P.; Álvarez, E. *Organometallics* **2007**, *26*, 1104.
(40) Lu, C. C.; Bill, E.; Weyhermüller, T.; Bothe, E.; Wieghardt, K. *J. Am. Chem. Soc.* **2008**, *130*, 3181.
(41) Lu, C. C.; Weyhermüller, T.; Bill, E.; Wieghardt, K. *Inorg. Chem.* **2009**, *48*, 6055.
(42) Bart, S. C.; Lobkovsky, E.; Chirik, P. J. *J. Am. Chem. Soc.* **2004**, *126*, 13794.
(43) Khorobkov, I.; Gambarotta, S.; Yap, G. P. A. *Organometallics* **2002**, *21*, 3088.
(44) Neese, F. *Orca an ab initio, DFT and Semiempirical Electronic Structure Package*, version 2.8, revision 2287; Institut für Physikalische und Theoretische Chemie, Universität Bonn: Bonn, Germany, November 2010.
(45) Noodleman, L.; Peng, C. Y.; Case, D. A.; Mouesca, J. M. *Coord. Chem. Rev.* **1995**, *144*, 199.
(46) Darmon, J. D.; Stieber, S. C. E.; Sylvester, K. T.; Fernández, I.; Lobkovsky, E.; Semproni, S. P.; Bill, E.; Wieghardt, K.; DeBeer, S.; Chirik, P. J. *J. Am. Chem. Soc.* **2012**, *134*, 17125.
(47) Trovitch, R. J.; Lobkovsky, E.; Chirik, P. J. *J. Am. Chem. Soc.* **2008**, *130*, 11631.
(48) Trovitch, R. J.; Lobkovsky, E.; Bouwkamp, M. W.; Chirik, P. J. *Organometallics* **2008**, *27*, 6264.
(49) Kleigrewe, N.; Steffen, W.; Blömker, T.; Kehr, Fröhlich, R.; Wibbeling, B.; Erker, G.; Wasilke, J.-C.; Wu, G.; Bazan, G. C. *J. Am. Chem. Soc.* **2005**, *127*, 13955.
(50) Small, B. L.; Brookhart, M.; Bennett, A. M. A. *J. Am. Chem. Soc.* **1998**, *120*, 4049.
(51) Stieber, S. C. E.; Milsmann, C.; Hoyt, J. M.; Turner, Z. R.; Finkelstein, K. D.; Wieghardt, K.; DeBeer, S.; Chirik, P. J. *Inorg. Chem.* **2012**, *51*, 3770.
(52) Gibson, V. C.; Humphries, M. J.; Tellmann, K. P.; Wass, D. F.; White, A. J. P.; Williams, D. J. *Chem. Commun.* **2001**, 2252.
(53) Knijnenburg, Q.; Hetterscheid, D.; Kooistra, T. M.; Budzelaar, P. H. M. *Eur. J. Inorg. Chem.* **2004**, 1204.
(54) Kaul, F. A. R.; Puchta, G. T.; Schneider, H.; Bielert, F.; Mihalios, D.; Herrmann, W. A. *Organometallics* **2002**, *21*, 74.

(55) Hayton, T. W.; Legzdins, P.; Sharp, W. B. *Chem. Rev.* **2002**, *102*, 935.
(56) Brunner, H.; Faustmann, P.; Nuber, B. *J. Organomet. Chem.* **1998**, *556*, 129.
(57) (a) Brunner, H.; Breu, J.; Faustmann, P. *Eur. J. Inorg. Chem.* **1998**, 1871. (b) Brunner, H.; Faustmann, P.; Bernhard, N. *J. Organomet. Chem.* **1999**, *579*, 1. (c) Lin, J. T.; Wang, S. Y.; Chou, Y. C.; Gong, M. L.; Shiow, Y. M.; Gau, H. M.; Wen, Y. S. *J. Organomet. Chem.* **1996**, *508*, 183.
(58) Schoffel, J.; Rogachev, A. Y.; De Beer Geoge, S.; Burger, P. *Angew. Chem., Int. Ed.* **2009**, *48*, 4734.
(59) Richter-Addo, G. B.; Legzdins, P. *Metal Nitrosyls*; Oxford University Press: New York, 1992.
(60) Ye, S.; Neese, F. *J. Am. Chem. Soc.* **2010**, *132*, 3646.
(61) Enemark, J. H.; Feltham, R. D. *Coord. Chem. Rev.* **1974**, *13*, 339.
(62) Bowman, A. C. Bis(imino)pyridine Iron and Cobalt Complexes: Preparation, Electronic Structure Determination and Reactivity of Metal-Ligand Multiple Bonds. Ph.D. Thesis, Cornell University, Ithaca, NY, February 2010.
(63) The generally accepted deviations between computed and experimental bond distances are 0.02−0.03 Å. The B3LYP functional is well known to overestimate M−L distances. See: Neese, F. *J. Biol. Inorg. Chem.* **2006**, *11*, 702.
(64) Tondreau, A. M.; Milsmann, C.; Patrick, A. D.; Hoyt, H. M.; Lobkovsky, E.; Wieghardt, K.; Chirik, P. J. *J. Am. Chem. Soc.* **2010**, *132*, 15046.
(65) Sieh, D.; Schlimm, M.; Andernach, L.; Angersbach, F.; Nuckel, S.; Schoffel, J.; Susnjar, N.; Burger, P. *Eur. J. Inorg. Chem.* **2012**, 444.
(66) Gallagher, M.; Wieder, N. L.; Dioumaev, V. K.; Carroll, P. J.; Berry, D. H. *Organometallics* **2010**, *29*, 591.
(67) Wang, S. G.; Qiu, Y. X.; Fang, H.; Schwarz, W. H. E. *Chem.—Eur. J.* **2006**, *12*, 4101.
(68) Milsmann, C.; Bill, E.; Weyhermüller, T.; George, S. D.; Wieghardt, K. *Inorg. Chem.* **2009**, *48*, 9754.
(69) Pangborn, A. B.; Giardello, M. A.; Grubbs, R. H.; Rosen, R. K.; Timmers, F. J. *Organometallics* **1996**, *15*, 1518.
(70) *Molekel*, Advanced Interactive 3D-Graphics for Molecular Sciences. Available under http://www.cscs.ch/molkel/.